View metadata, citation and similar papers at core.ac.uk

brought to you by CORE

provided by Aaltodoc Publication Archive

Aalto University

Colloidal structures of phospholipids in vegetable oil and their potential usage in surface treatment of nanocellulose for food applications

Olli-Pekka Lehtinen

Licentiate thesis

Bioproduct technology

Date: 16.6.2019

Supervisor: Professor Orlando Rojas

Advisors: Ph.D. Long Bai, D.Sc. (Tech.) Sanna Hokkanen

Aalto University

School of Chemical Engineering

Department of Bioproducts and Biosystems

Biobased Colloids and Materials

Aalto University

Aalto University, P.O. BOX 11000, 00076 AALTO
www.aalto.fi

Abstract of licentiate thesis

Author	Olli-Pekka Lehtinen
Title of thesis	Colloidal structures of phospholipids in vegetable oil and their potential usage in surface treatment of nanocellulose for food applications
Department	Department of Bioproducts and Biosystems
Field of research	Bioproduct technology
Supervising professor	Professor Orlando Rojas
Thesis advisor(s)	Ph.D. Long Bai, D.Sc. (Tech.) Sanna Hokkanen
Thesis examiner(s)	Assistant Professor Kirsi S. Mikkonen, Ph.D. Carlos Rodriguez-Abreu
Number of pages	48
Language	English
Date of submission for examination	16.6.2019

Abstract

The aim of the licentiate's thesis was to understand the colloidal behaviour of phospholipids in vegetable oils and to study the adsorption of phospholipid nanostructures onto the surface of cellulose nanofibrils.

Water concentration, temperature and free fatty acid had an effect on the formation of reverse micelles of phospholipids in vegetable oil. At low water concentration, phospholipids formed solubilized reverse cylindrical micelles above critical micelle concentration (*cmc*) in the oil. Increasing temperature decreased the *cmc* of phospholipids in oil. Addition of moderate amount of water into oil caused solubilized phospholipids to form lamellar liquid crystal structures that were precipitated from the oil and formed separate phase. Oleic acid in rapeseed oil increased the solubility of lecithin and suppressed the formation of phospholipid reverse micelles at low water content. In presence of more water, the oleic acid stabilized the reverse micelles and consequently more water was needed to induce the phase separation. Thus it could be concluded that moderate amounts of oleic acid (5 wt.-%, 10 wt.-% and 20 wt.-%) in the oil delayed the removal of phospholipid reverse micelles upon addition of water, and the formation of lamellar structures required more water. This was caused by the increased solubility of lecithin into oil due to the co-solvent effect of oleic acid.

Nanocellulose has shown many potential applications in foods, such as emulsifiers, fillers, structuring agents and cholesterol binders. An interesting application for nanocellulose would be the replacement of saturated fats in foods to decrease the fat content and the energy content of the products. To increase the compatibility of nanocellulose with the vegetable oil, the adsorption of phospholipid nanostructures was studied by immersing cellulose nanofibril film into the oily liquid containing phospholipid lamellar structures.

The contact angle measurement seemed not to be an optimal way to measure the adsorption of phospholipids onto the surface of nanocellulose due to the variation in the results. Some of the contact angle measurement results indicated that the addition of the oily liquid containing phospholipid lamellar structures onto the surface of nanocellulose decreased the hydrophilicity of the surface after rinsing it with chloroform. In addition, two measurements indicated that the addition of oily liquid containing phospholipid lamellar structures decreased the hydrophilicity of the surface.

Keywords Reverse micelles, phospholipids, vegetable oil, free fatty acid, cellulose nanofibrils,

Aalto-yliopisto

Aalto-yliopisto, PL 11000, 00076 AALTO
www.aalto.fi

Lisensiaatin tutkimuksen tiivistelmä

Tekijä Olli-Pekka Lehtinen

Työn nimi Fosfolipidien kolloidaaliset rakenteet kasviöljyssä ja niiden mahdollinen käyttö nanoselluloosan pintakäsittelyssä elintarvikesovellutuksiin

Laitos Biotuotteiden ja biotekniikan laitos

Tutkimusala Biotuoteteknologia

Vastuuprofessori Professori Orlando Rojas

Työn ohjaajat Ph.D. Long Bai, TkT Sanna Hokkanen

Työn tarkastajat Apulaisprofessori Kirsi S. Mikkonen, Ph.D. Carlos Rodriguez-Abreu

Jätetty tarkastettavaksi 16.6.2019 **Sivumäärä** 48 **Kieli** Englanti

Tiivistelmä

Lisensiaatin työn tarkoituksena oli ymmärtää fosfolipidien kolloidaalista käyttäytymistä kasviöljyissä sekä tutkia fosfolipidien muodostamien nanorakenteiden kiinnittymistä selluloosananofibrillien pintaan.

Vesipitoisuudella, lämpötilalla ja vapailla rasvahapoilla oli vaikutus käänteisten fosfolipidimisellien muodostumiseen kasviöljyssä. Matalassa vesipitoisuudessa fosfolipidit muodostivat liukoisia käänteisiä sylinterinmuotoisia misellejä kriittistä misellipitoisuutta (*cmc*) korkeammassa pitoisuudessa öljyssä. Lämpötilan nousu madalsi fosfolipidien *cmc*:tä öljyssä. Kohtuullisen vesimäärän lisäys öljyyn sai liukoiset fosfolipidit muodostamaan lamellaarisia nestekristallirakenteita jotka saostuivat öljystä ja muodostivat erillisen faasin. Oleiinihappo rypsiöljyssä nosti lesitiinin liukoisuutta ja madalsi fosfolipidien käänteisten misellien muodostusta matalassa vesipitoisuudessa. Korkeammassa vesipitoisuudessa oleiinihappo tasapainotti käänteisiä misellejä ja sen seurauksena enemmän vettä tarvittiin käynnistämään faasien erottuminen. Näin ollen voitiin päätellä, että kohtalaiset oleiinihappomäärät (5 paino-%, 10 paino-% ja 20 paino-%) öljyssä hidastivat fosfolipidien käänteisten misellien poistamista veden lisäyksessä ja lamellaaristen rakenteiden muodostuminen vaati enemmän vettä. Tämä johtui lesitiinin suuremmasta liukoisuudesta öljyyn jonka aikaansai oleiinihapon yhteisliuotusvaikutus.

Nanoselluloosalla on monia potentiaalisia sovellutuksia elintarvikkeissa kuten emulgaattoreina, täyteaineina, rakenneaineina ja kolesterolin sitojina. Yksi kiinnostava sovellutus nanoselluloosalle olisi tyydyttyneiden rasvojen korvaamisessa elintarvikkeissa vähentämään tuotteiden rasvapitoisuutta ja energiapitoisuutta. Lisätäkseen nanoselluloosan yhteensopivuutta kasviöljyn kanssa, fosfolipidinanorakenteiden kiinnittymistä tutkittiin kastamalla selluloosananofibrillikalvo öljyiseen nesteeseen joka sisälsi fosfolipidien lamellaarisia rakenteita.

Kontaktikulmamittaus ei vaikuttanut olevan paras tapa mitata fosfolipidien kiinnittymistä nanoselluloosan pintaan tulosten suuren hajonnan vuoksi. Eräät kontaktikulmamittaustulokset osoittivat että fosfolipidien lamellaarisia rakenteita sisältävän öljyisen nesteen lisäys nanoselluloosan pinnalle vähensi pinnan hydrofiilisyyttä sen jälkeen kun se huuhdeltiin kloroformilla. Lisäksi kaksi mittausta osoitti että fosfolipidejä sisältävän öljyisen nesteen lisäys vähensi pinnan hydrofiilisyyttä.

Avainsanat käänteiset misellit, fosfolipidit, kasviöljy, vapaat rasvahapot, selluloosananofibrillit

Preface

The work presented in the thesis was conducted between June 2015 and October 2019. I would like to express my thanks to Professor Orlando Rojas, Ph.D. Long Bai and D.Sc. (Tech.) Sanna Hokkanen. I would also like to thank other authors in the thesis article (publication).

Klaukkala, Finland, 15th October 2019

Olli-Pekka Lehtinen

List of abbreviations

BC	Bacterial cellulose
CA	Contact angle
cmc	Critical micelle concentration
CMF	Cellulose microfibrils
CNC	Cellulose nanocrystals
CNF	Cellulose nanofibrils
Cryo-TEM	Cryogenic transmission electron microscopy
FFT	Fast Fourier Transform
H_α	Hexagonal crystals with liquid like chains
LB	Langmuir-Blodgett
LP	Lecithin precipitate
L_α	Lamellar liquid crystals with liquid like chains
L_β	Lamellar crystals with stiff chains
MFC	Microfibrillated cellulose
o/w	Oil-in-water
PEI	Poly(ethyleneimine)
POPC	Palmitoyl-oleoyl-phosphatidyl choline
POPE	Palmitoyl-oleoyl-phosphatidyl ethanolamine
Q_α	Cubic crystals with liquid like chains
SAXS	Small-angle X-ray scattering
SPI	Soybean protein isolate
TCNQ	7,7,8,8–tetracyanoquinodimethane dye
w/o	Water-in-oil
w_0	Water/lecithin molar ratio

Author Contributions

Published paper: Olli-Pekka Lehtinen was responsible for the planning of the work and experimental design together with other authors mainly Tuula Lehtimaa and Monika Österberg. The preliminary laboratory work related to sample preparation including the preparation of the samples, material drying, solubilization experiments and Karl-Fischer analyses were done by Olli-Pekka Lehtinen. The designing of the preliminary experiments was done mainly by Olli-Pekka Lehtinen, Tuula Lehtimaa and Monika Österberg. Olli-Pekka Lehtinen conducted the experimental design for TCNQ method and performed the TCNQ method experiments and analyzed the results of the TCNQ method. The results of the TCNQ method were critically reviewed mainly by Olli-Pekka Lehtinen, Monika Österberg and Tuula Lehtimaa. Planning of the cryo-TEM imaging and SAXS measurement experiments was done by Olli-Pekka Lehtinen, Tuula Lehtimaa and Monika Österberg. The experimental design for both cryo-TEM imaging and SAXS measurements was done by Olli-Pekka Lehtinen. Janne Ruokolainen performed the cryo-TEM imaging including the vitrification of the samples and Olli-Pekka Lehtinen was responsible of the sample preparation. The results of the cryo-TEM imaging were analyzed by Olli-Pekka Lehtinen together with Janne Ruokolainen. Janne Ruokolainen also guided in the performance of the analysis. Robertus Wahyu N. Nugroho contributed in the sample preparation of the cryo-TEM imaging and analysis of the cryo-TEM imaging results in late experiments. Panu Hiekkataipale performed the SAXS measurements and Olli-Pekka Lehtinen was responsible of the sample preparation and the preparation of the SAXS samples into holders. Panu Hiekkataipale guided in the preparation of the SAXS samples. The results of the SAXS measurements were analyzed by Olli-Pekka Lehtinen together with Panu Hiekkataipale. Panu Hiekkataipale guided in the performance of the analysis. Robertus Wahyu N. Nugroho contributed in the SAXS measurements and the analysis in the late experiments. The results of the cryo-TEM imaging and the SAXS measurements were critically reviewed mainly by Olli-Pekka Lehtinen, Tuula Lehtimaa and Monika Österberg. Also Robertus Wahyu N. Nugroho contributed to the reviewing of the results of SAXS measurements and cryo-TEM imaging in late experiments. Sampsa Vierros and Maria Sammalkorpi were responsible for the computer simulation work. Robertus Wahyu N. Nugroho and Olli-Pekka Lehtinen wrote the manuscript together with the other authors under supervision of Monika Österberg.

Table of contents

1. Introduction

Nanomaterials have potential to enhance the food and beverage production and products. However, novel nanomaterials have not been used directly in human foods. The only exception is food pigment titanium dioxide and food colorant iron oxide (He *et al*., 2019). Nanotechnology refers to the technology that deals with materials which have at least one dimension in nanometer-scale. Nanocellulose has potential to be used to produce low-fat food products and to reduce their energy density. One of the interesting applications for nanocellulose is the replacement of saturated fats that are part of an atherogenic diet (high in saturated fats and low in vegetables, fruits, and whole grain), which was one of the major risk factors for cardiovascular disease, namely coronary heart disease (Rolfes *et al.*, 2009). The saturated fat replacement can be applied in food products such as in salad dressings, bakery products and chocolate products by using a combination of low-calorie, plant-based nanocellulose and lipids, more specific phospholipids. The fat-replacer should have similar textural properties as the saturated fat such as firmness and mouthfeel. Depending on the consumer product, the temperature profile should allow melting at mouth temperature.

Nanocellulose has hydrophilic surface due to the functional groups (e.g. hydroxyl groups). This limits its compatibility with hydrophobic food matrices such as vegetable oils. A potential way to decrease the hydrophilicity of nanocellulose would be the adsorption of amphiphilic phospholipids onto the surface. The hydrophilic head groups of the phospholipids would be adsorbed onto the surface of nanocellulose leaving the hydrophobic tails of the phospholipids exposed to the surroundings. Phospholipids are food grade ingredients, and thus they are excellent for covering the surface of nanocellulose for food applications.

The aim of the thesis is to understand the colloidal properties of phospholipids in vegetable oils that affect their usage in applications such as plant oils, emulsifiers and oleogels and to discuss about food applications of nanocellulose. The combination of phospholipids and nanocellulose was studied in order to establish the starting point for the usage of nanocellullose as food additive in lipid environments.

2. Literature

2.1. Phospholipids

Phospholipids are sometimes referred as polar lipids as they are composed of polar head group and hydrophobic hydrocarbon tails. Phospholipids are constituents of cell membranes, and active participants in metabolic processes. Phospholipids are concentrated in the organs such as the brain, liver and kidney in human and animals, and in plants the amount is highest in seeds, nuts and grains (Szuhaj, 2005). Phospholipids are constituents of serum lipoproteins (Oncley and Harvie, 1969) and part of the bladder bile (Isaksson, 1951). There are two main groups of phospholipids: the glycerophospholipids that are derived from glycerol and the sphingophospholipids that are derived from sphingosine. The glycerophospholipids are derivatives of glycero-phosphoric acid. They contain hydrophilic group and one or two *O*-acyl, *O*-alkyl or *O*-(1-alkenyl) chains attached to the glycerol. The sphingophospholipids contain group R and R´. The most common sphingophospholipid is sphingomyelin in which the R is replaced by $-CH_2CH_2N^+(CH_3)_3$ (choline) (Walde *et al.*, 1990). Phosphoglycerides are closely related to fats and oils in that they contain a glycerol backbone linked by ester bonds to two fatty acids and one phosphoric acid. The phosphate group at C3 is also bonded by an ester link to an amino alcohol such as choline (in phoshatidylcholine, a lecithin) or ethanolamine (in phosphatidylethanolamine, a cephalin). The sphingolipids have sphingosine or a related dihydroxyamine as their backbones and are constituents of plant and animal cell membranes. Sphingolipids are particularly abundant in brain and nerve tissue, where compounds called sphingomyelins are major constituent of the coating around nerve fibers. (McMurry and Simanek, 2007)

Phospholipids can be divided into four classes according to their water-solubility. The first class was the water-insoluble phospholipids that did not adsorb water (e.g. waxes). The second class was the phospholipids with low water-solubility that swell in presence of water (e.g. long-chain phosphatidylcholine, phosphatidylethanolamine or sphingomyelin). The third class included water-soluble phospholipids, which could be divided into two subclasses. The first subclass consisted of water-soluble phospholipids that formed lyotropic liquid crystals at low water content (e.g. lysolecithins). The second subclass consisted of the water-soluble phospholipids that formed micelles in water above critical micelle concentration (*cmc*) while not forming crystalline structure (e.g. saponins). (Pichot *et al.* 2013)

Lecithin is a commonly used phospholipid rich material. According to Szuhaj (2005), the term lecithin referred to a complex, naturally occurring mixture of polar lipids obtained by water-degumming of crude vegetable oils and separating and drying the hydrated gums. According to the

author, the phospholipid portion of lecithin was mainly responsible for giving form and function to commercial lecithin. The phospholipid composition of soy and egg lecithin presented differences, as shown in Table 1. The author also reported that the plant/legume (e.g. soy) had higher unsaturated fatty acid content compared to the lecithin in egg yolk and no cholesterol. McMurry and Simanek (2007) reported that the fatty acid residues in phosphoglycerides could be any of the C_{12}–C_{20} units, and the acyl group at C1 was usually saturated and that at C2 was usually unsaturated. The fatty acid compositions of soy and egg are shown in Table 2.

Table 1. Composition of soy lecithin and egg lecithin (Adapted from Szuhaj, 2005)

Polar lipids	Soy	Egg
Phosphatidylcholine	20–22	68–72
Phosphatidylethanolamine	21–23	12–16
Phosphatidylinositol	18–20	0–2
Phosphatidic acid	4–8	-
Sphingomyelin	-	2–4
Other phospholipids	15	10
Glycolipids	9–12	-

Table 2. Fatty acid composition (%) (Adapted from Szuhaj, 2005)

Type of acid	Soy	Egg
Saturated		
Palmitic	15–18	27–29
Stearic	3–6	14–17
Unsaturated		
Oleic	9–11	35–38
Linoleic	56–60	15–18
Linolenic	6–9	0–1
Arachidonic	0	3–5

2.1.1. Water adsorption of phospholipids

Phospholipids form different structures depending on the water-to-phospholipid ratio (w/w). For example Lei *et al.*, (2003) reported that the effective head group area of the phospholipid was enlarged by increasing the water concentration in phospholipid-soybean oil system due to the swelling of the phospholipid that led to the formation of insoluble phospholipid aggregates. According to Hauser *et al.* (1981) the polar region of the phospholipid consisted of three parts: the head group (e.g. choline), the glycerol moiety and two carboxylic ester groups. Jendrasiak *et al.* (1996) reported that water adsorbed to the polar head group of phospholipid caused rearrangement of the lipid molecular organization upon hydration or dehydration. The water

adsorption characteristics were dependent on the total head group structure including hydrophobic moieties and the electrical charge of the head group. Depending on the phospholipid type, the water adsorption capacity ranged from 6.5 to 100 water molecules per one phospholipid molecule. For example, total 9 water molecules was adsorbed by per L-α-dipalmitoyl-phosphatidylcholine molecule, 17 water molecules per L-α-dioleoyl-phosphatidylcholine molecule and 21.5 water molecules per L-α-dilinoleoyl-phosphatidylcholine molecule. Water hydration of phosphatidylcholine was reported to increase with increasing number of double bonds in the hydrocarbon chains and with bound cholesterol. It was shown that three different types of water were adsorbed with the phospholipid molecules: (1) tightly bound water, (2) intermediately bound water and (3) free water. However, only one type of adsorbed water before the free water zone was reported for egg phosphatidylethanolamine, egg lyso-phosphatidylethanolamine, bovine phosphatidylserine and bovine lyso-phophatidylserine (Jendrasiak and Hasty 1974 and Jendrasiak *et al.*, 1996). The water adsorption capacities of some phospholipid as well as other lipids are shown in Table 3.

Table 3. Number of adsorbed water molecules per phospholipid molecule at 22 °C. (Adapted from Jendrasiak and Hasty, 1974 and Jendrasiak *et al.*, 1996)

Phospholipid	**Water molecules**
Egg phosphatidyl choline	13.5
Egg lyso-phosphatidyl choline	17.0
Cholesterol	1.0
Egg phosphatidyl choline- cholesterol complex (1:1) mol	18.8
Dipalmitoyl phosphatidyl choline	9.0
Dioleoyl phosphatidyl choline	17.0
Dilinoleoyl phosphatidyl choline	21.5
Egg phosphatidyl ethanolamine	9.0
Egg lyso-phosphatidyl ethanolamine	10.0
Bovine phophatidyl serine	6.5
Bovine lyso-phosphatidyl serine	100.0
Bovine heart cardiolipin	36.0
Egg phophatidic acid	14.7
Egg phosphatidyl choline-phosphatidic acid complex (7:4 M/M)	17.0

2.1.2. Phospholipid structures in nonpolar liquids

Water-to-phospholipid ratio (w/w) can be used to control the phospholipid self-aggregation in vegetable oil. The water-to-phospholipid ratio affects the shape of the phospholipid aggregates (Table 4). The phospholipid structures described in the literature were phospholipid spherical reverse micelles (Elworthy, 1959), cylindrical reverse micelles (Schurtenberger *et al.*, 1990), lamellar structures, reverse hexagonal phase, cubic liquid-crystalline phase (Angelico *et al.*, 2000), spheroidal reverse micelles (Danino *et al.*, 2002) and rodlike reverse micelles. (Cirkel and Koper, 1998)

Table 4. Colloidal phospholipid structures in nonpolar solvents. (Elworthy, 1959, Gupta *et al.*, 2001, Subramanian *et al.*, 2001, Danino *et al.*, 2002, Angelico *et al.*, 2000, Schurtenberger *et al.*, 1990, Cirkel and Koper, 1998, Angelico *et al.*, 2000, Lei *et al.*, 2003)

Colloidal structure	**Amount of water**	**Amount of phospholipid**	**Reference**
Smaller and larger reverse micelles	~0 wt.-%	0.083 wt.-%	Elworthy, 1959
Spherical reverse micelles (size = 0.70 nm)	0.30 %	5 %	Gupta *et al.*, 2001
Reverse micelles (Diameter = 3.56 nm)	0.07 wt.-%	0.89 wt.-%	Subramanian *et al.*, 2001
Spheroidal reverse micelles	~0 %	5 %	Danino *et al.*, 2002
Reverse hexagonal phase	Max. ~40 wt.-%	34-77 wt.-%	Angelico *et al.*, 2000
Reverse hexagonal lyotropic liquid crystalline phase	~0 wt.-%	1.7 %	Danino *et al.*, 2002
Cylindrical reverse micelles	Vary (For example at ~1.23 wt.-%)	Vary (For example ~17.64 wt.-%)	Schurtenberger *et al.*, 1990
Rodlike reverse micelles	Vary	Vary	Cirkel and Koper, 1998
Reverse wormlike aggregates	Vary	Vary	Angelico *et al.*, 2000
Cubic Liquid-Crystalline phase	Vary	Vary	Angelico *et al.*, 2000
Lamellar phase	Max. 45 wt.-%	50-100 wt.-%	Angelico *et al.*, 2000
Lamellar phase	Vary	Vary	Lei *et al.*, 2003

2.1.2.1. Phospholipid spherical reverse micelles

The first group of phospholipid aggregates is phospholipid reverse micelles (Figure 1) that had been reported to be present at low water concentration. The shape of the reverse phospholipid micelles is spherical (Gupta *et al.*, 2001) or spheroidal, that is approximately spherical (Danino *et al.*, 2002). A study of Kanamoto *et al.*, 1981 reported that phospholipids aggregated into reverse micelles in vegetable oils at concentration above the *cmc* at very low water concentration. They also reported that the *cmc* of phospholipids decreased with increasing hydrophilicity of the polar head group due to the polar-non-polar interactions between the oil phase and polar headgroup. For example, the *cmc* of phosphatidyl choline, phosphatidyl ethanolamine and phosphatidic acid were reported to be 0.085 mM, 0.84 mM and 2.6 mM in soybean oil, respectively. A study of Cui *et al.*, 2014 reported that an increase in temperature from room temperature to 45 °C decreased the *cmc* of 1,2-Dioleoyl-*sn*-glycero-3-phosphocholine and 1,2-Dioleoyl-*sn*-glycero-3-phosphoethanolamine from 50 µM to 20 µM and from 800 µM to 200 µM, respectively.

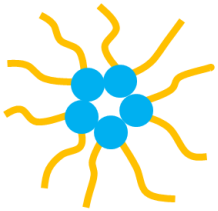

Figure 1. Illustration of phospholipid spherical reverse micelle inspired by Gupta *et al.* (2001)

Subramanian *et al.*, 2001 reported that phospholipid reverse micelles were present in vegetable oil systems with traces of water or slightly more. Elworthy (1959) pointed out that dried lecithin was transferred into dry benzene and reverse micelles were formed. However, the study did not prove experimentally that the lecithin and the solvent were anhydrous. Thus, it remains unclear whether phospholipid reverse micelles could form in anhydrous conditions. The size of reverse phospholipid micelles was smaller at low water concentrations as minimal water was present pool inside the micelles. The diameter of reverse phospholipid micelles was reported to be between 5.0 to 9.2 nm at 24 °C in varying ratios of hexane-oil mixture. The reverse phospholipid micelles were able to take up some water which caused them to swell. The water was presumably adsorbed into the small water pool inside the reverse phospholipid micelle surrounded by the polar head groups. The size of the reverse micelles increased from 7.0 to 8.7 nm when water concentration increased from 0.3 to 1.5 wt.-% in system with 5 % phospholipids in hexane-soybean oil (70/30) mixture. Correspondingly, the water-to-phospholipid ratio increased from 0.06 to 0.30 (Gupta *et al.*, 2001). On the other hand, the authors reported that an increase in temperature from 24 to 65 °C had an

insignificant effect on the size of micellar aggregates of phospholipids in soybean oil-hexane solution, yet generally smaller micellar aggregates were reported at 65 °C. Size increasing trend was also reported in a study of Subramanian *et al.* (2001) in which the diameter of reverse micelles of phospholipids increased from 3.56 to 4.60 nm when the water-to-phosphatidylcholine ratio increased from 0.079 to 0.112 in system with 8900 mg/kg (0.89 wt.-%) phosphatidylcholine in triolein. The size of the reverse phospholipid micelles also increased with increasing phospholipid concentration. When phosphatidylcholine concentration increased from 0.89 to 1.77 %, the diameter of reverse phospholipid micelles increased from 3.56 nm to 3.70 nm in triolein with 700 mg/kg water. The diameter increased from 4.22 to 4.70 nm in triolein when the increase in phosphatidylcholine concentration was much higher (from 4.52 to 9.13 %) at constant water concentration of 600 mg/kg.

2.1.2.2. Phospholipid cylindrical reverse micelles

The second group of phospholipid structures is elongated cylindrical reverse micelles (Figure 2). These structures have been reported to be present in several organic solvents, including cyclohexane, isooctane and *n*-decane. Such cylindrical reverse micelles were formed when small amount of water was added to the phospholipid-isooctane system (Schurtenberger *et al.*, 1990). According to a study of Imai *et al.* (2013), water molecules attached to the phosphate group of the neighboring phospholipids in spherical reverse micelles through hydrogen bonding. This increased the volume of the polar head group and thus reduced the interface curvature of the reverse micelles. As a result, spherical or ellipsoidal reverse micelles elongated into long and narrow reverse cylindrical micelles showing worm-like appearance. Palazzo (2013) reported that the length and branching of the cylindrical reverse micelles were controlled by a delicate energy balances between the micelle endcaps and the branches.

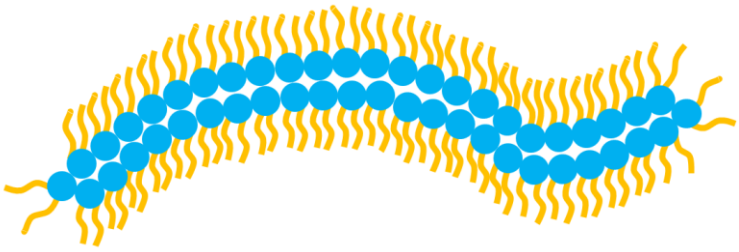

Figure 2. Illustration of phospholipid cylindrical reverse micelle.

Imai *et al.* (2013) reported that cylindrical reverse micelles entangled to each other and formed a three-dimensional network within the oil. A study of Palazzo (2013) explained that the cylindrical micelles were under thermodynamic control and their contour length distribution was not fixed by chemical synthesis as was in polymer networks. The contour length varied reversibly with concentration and temperature. The entanglement induced a transformation from liquid oil to an organogel with viscosity up to few thousands poise (Scartazzini and Luisi, 1988). A study of Schurtenberger *et al.* (1990) reported an increase of zero shear viscosity of 200 mM soybean lecithin in isooctane system when small amounts of water were added to the system at 20 °C. The authors reported that the zero shear viscosity of the system increased by more than a factor of 10^6 when the water/lecithin molar ratio (w_0) increased from 0 to 3 by addition of water from the syringe. Further increase of w_0 from 3 to above 5 decreased the zero shear viscosity. At $w_0 > 5$, the system separated into two macroscopical phases that were optically clear.

2.1.2.3. Phospholipid lamellar structures

Phospholipids may form lamellar liquid crystals with liquid like chains (L_α) in presence of water (Small, 1986). Water changes the phospholipid structures from isotropic liquid phase (L_2 phase) into lamellar structures that are insoluble in oil (Lei *et al.*, 2003). The phospholipid lamellar structure is illustrated in Figure 3. According to Angelico *et al.* (2000) the contour length of the wormlike micelles increased with increasing the value of water/lecithin molar ratio (w_0) up to 10-12. The cylindrical reverse micelles had high aspect ratio. When w_0 increased to moderate values (13-15), the cylindrical reverse micelles were present together with swollen spherical micelles. When more water was added, the spherical reverse micelles dominated the system up to the phase separation into third phase that was a lamellar phase. At higher water concentrations, an aqueous phase separated. Similar phenomenon was also reported in a study of Lei *et al.* (2003) with water saturation level of phospholipid lamellar phase around 40 %.

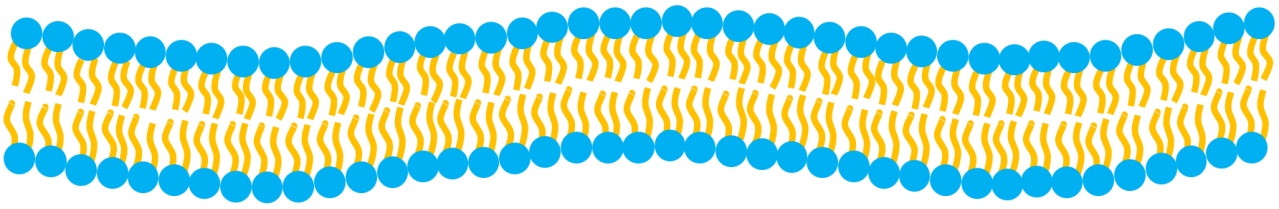

Figure 3. Illustration of phospholipid lamellar structure.

Several studies describe the characteristics of the phospholipid bilayer structure measured from crystallized phospholipid material at low water content. Hauser *et al.*, (1980) reported that the 3-

dodecanoyl-propandiol-1-phosphorylcholine · H_2O bilayer structures had a close resemblance to the gel state of lysophosphatidyl choline and diacylphosphatidyl choline, which would allow the interpretation of the molecular conformational and packing principles of the fully hydrated lamellar structures of membrane lipids. In the same study, the authors also claimed that the phospholipid lamellar structures were formed both in presence and absence of water.

According to Pascher *et al.* (1981) the 3-palmitoyl-DL-glycerol-1-phosphorylethanolamine or lysophosphatidyl ethanolamine molecules packed in a bilayer arrangement in a solid crystalline form. The phosphatidyl ethanolamine groups had an orientation parallel to the layer of the surface. The packing consisted of unit cells. The unit cell contained four molecules, two enantiomers on each layer side. The unit cell dimensions were 7.66, 9.08 and 37.08 Å in *a*, *b*, and *c* directions, respectively, where the latter one represented the bilayer thickness. The *a* and *b* direction were along the bilayer surface and perpendicular to each other. The *c* direction was perpendicular to the bilayer surface. Each head group took an area of 34.8 $Å^2$ in the bilayer surface. The cross-section of each hydrocarbon chain perpendicular to its long axis had a size of 18.7 $Å^2$. Hydrocarbon chains had an extremely large tilt angle (57.5°) with respect to the layer normal because they had to accommodate the much larger area of the head groups. The angle of the tilt was close to the maximum that chains could have in bilayer structure. In the case that the area per head group increased to twice the area of cross-section of the hydrocarbon chains, the hydrocarbon chains would interdigitate with the opposite layer. However, this was not the case with 3-palmitoyl-DL-glycerol-1-phosphorylethanolamine or lysophosphatidyl ethanolamine. The phosphorylethanolamine groups were linked to each other by hydrogen-bond system. The lateral packing of the molecules was indirectly affected by the free glycerol hydroxyl group that formed an intramolecular hydrogen bond (2.80 Å) with the unesterified phosphate oxygen that affected the conformation and orientation of the phosphorylethanolamine group. The intermolecular bonds were formed between the molecules involving three hydrogen atoms in the ammonium group of molecules and unesterified phosphate oxygen atom in the neighbouring molecules. Each ammonium group formed two bonds to lateral neighbor molecules in *a* and *b* directions and one bond to a molecule of the next bilayer in the *c* direction. The headgroups of different enantiomers were linked into double rows by the hydrogen bonds extending in the *ab* plane. In lateral direction, there were no hydrogen bonds between the double rows of phosphatidyl ethanolamine groups. In the adjacent bilayer surface, the head groups were located so that the double rows were located over the gaps. The linkage between the double rows was induced by the hydrogen bonds across the layer surface.

According to Small (1986) both water concentration and temperature had an effect on the L_α consisting lecithin. L_α phase was reported to occur in lecithin-water system with water concentration above 10-20 wt.-% depending on temperature. Above 10-20 wt.-% water

concentration, L_α phase was present in temperature range from approximately 2 to 225 °C. When water concentration was increased above 40-44 wt.-% a second phase appeared in the system. At lower water concentration, lecithin was reported to form different crystalline phases, for instance, lamellar crystals with stiff chains (L_β), crystalline lecithin, cubic crystals with liquidlike chains (Q_α), rhombohedric crystals with liquid like chains, and hexagonal crystals with liquid like chains (H_α). At higher temperature (>220-232 °C) lecithin crystals would melt to an isotropic liquid below approximately 35 wt.-% water concentration. The isotropic liquid phase coexisted with water phase if there was more water present at the elevated temperatures.

2.1.3. Phase separation of phospholipids

Phase separation of solubilized phospholipids from vegetable oil is an important phenomenon because it is a potential way to produce phospholipid lamellar structures. The separation of phospholipid from vegetable oil could be carried out by adding moderate amount of water into the system. The formation of lecithin lamellar structures in vegetable oil was discussed in detail in the publication. (Lehtinen *et al.*, 2017)

A study of Angelico *et al.* (2005) reported that with water loadings above critical hydration resulted in a phase separation between a birefringent liquid-crystalline phase and a less dense isotropic phase in system that composed of lecithin in isopropylpalmitate and ethyloleate. The phase boundary was reported to occur at w_0 of ~5.2 for isopropylpalmitate with total lecithin concentration 5 % and 15 %. In ethyloleate, the phase boundary was reported to occur at w_0 of ~6.6 with total lecithin concentration 5 %. The isotropic phase was reported to be not very viscous and contained lecithin and water. The dense phase was reported to reveal the same textures as usually associated with a lamellar phase according to crossed polarizer and small-angle X-ray scattering (SAXS) spectra.

Studies of Lei *et al.* (2003) and Angelico *et al.* (2000) reported that the phase separation of the phospholipid-vegetable oil-water system occurred at water saturation approximately 40 %. This was seen as a phase separation of 2-phase system of soluble phospholipid reverse micelles and vegetable oil into a 3-phase system of insoluble phospholipid liquid crystals, vegetable oil and water phase. The precipitate of lecithin consisted of lamellar phospholipid structures and the effective head group area of the phospholipid was enlarged by increasing the water concentration in phospholipid-soybean oil system due to the swelling of the phospholipid that lead to the formation of insoluble colloidal phospholipid aggregates. (Lei *et al.*, 2003)

2.2. Motivation for nanocellulose-phospholipid applications

Nanomaterials have been researched as emulsifiers, fillers and cholesterol binders for food applications. An interesting nanomaterial is the plant-based nanocelluloses that are extracted from wood, cotton, natural fibers and lignocellulosic materials. Nanocellulose has been widely used to manufacture a range of different cellulose-based nanomaterials that are one-dimensional in the nanometer range. These include whiskers, microfibrillated cellulose, nanofibrillated cellulose and cellulose nanofibrils or microfibrils. (Gómez *et al.*, 2016)

The surface of nanocellulose is hydrophilic due to the large amount of hydroxyl groups. The hydrophilicity of the surface generates repulsion towards hydrophobic vegetable oil. A potential way to modify the surface of nanocellulose would be the adsorption of surfactants onto the surface. Surfactants usually consist of both hydrophilic head group and hydrophobic tail. The hydrophilic head groups would be adsorbed onto the hydrophilic groups of nanocellulose having the hydrophobic tail exposed to the surroundings. This would render the outer most surface and reduce the repulsion towards the vegetable oil. Potential surfactants for surface modification are food grade phospholipids from natural sources (e.g. soy or egg). Certain phospholipid structures, such as lamellar phospholipid structures, have beneficial orientation so that the hydrophilic groups are readily exposed for adsorption onto the nanocellulose surface.

2.2.1. Properties of nanocellulose

Nanocellulose can be produced from lignocellulosic material (e.g. wood) or as a product from micro-organisms (e.g. bacterial cellulose). Different types of nanocellulose include microfibrillated cellulose (MFC), cellulose nanocrystals (CNC) and bacterial nanocellulose (BC). Dufresne (2012) reported that the hierarchical structure of natural fibers could be disintegrated using a top-down deconstruction method by mechanically submitting slurries of cellulose fibers to high shearing forces. This produced MFC that was composed of nanosized cellulose fibrils with a high aspect ratio. The microfibrils or microfibril bundles showed diameters in the order of 10-100 nm and the length could be in the micrometer scale. There were alternative terms used in the literatures to describe the MFC including cellulose microfibrils (CMF), cellulose nanofibers, cellulose nanofibrils (CNF), nanofibrillated cellulose, and microfibrillar cellulose. Bleached pulps can be used to produce MFC and otherwise it is necessary to submit the material to a purification step using chemical treatments to remove the non-cellulosic components. The preparation of second type of nanocellulose, CNC, involved a chemical acid hydrolysis process to dissolve amorphous chains from the cellulose fibers and to release crystal domains that remain intact after acid hydrolysis. Fibers are first alkali treated and bleached followed by hydrolysis with H_2SO_4 or HCl reflux. The

material is then purified through dialysis following with sonication to obtain CNC. In the acid hydrolysis treatment, the amorphous regions surrounding and embedded within CMF were disrupted. During the acid hydrolysis process, the hydronium ions could penetrate the cellulose chains in the amorphous domains and promoted the hydrolytic cleavage of the glycosidic bonds and released individual crystallites. Different terminology used in the literature to refer the crystalline rod-like nanoparticles included cellulose nanocrystals, cellulose nanowhiskers or nanocrystalline cellulose to name the few. Third type of nanocellulose could be produced as microbial extracellular polymer called bacterial cellulose or microbial cellulose. It belongs to specific products of primary metabolism and constitutes mainly a protective coating. The most studied and used bacterium species for production of BC was *Acetobacter xylinum*, formerly known as *Acetobacterium xylinum* and *Bacterium xylinodes*, reclassified as the genus *Gluconacetobacter*. One of the important features of BC is the chemical purity that distinguished it from the plant-based cellulose that was usually associated with lignin and hemicelluloses. BC is associated with the production of vinegar, Kombucha tea and the Philippine dessert, nata de coco.

Nanocellulose can be used as an emulsifier due to its amphiphilic properties. Nanocelluloses can produce oil-in-water (o/w) Pickering emulsions. Nanocelluloses can also produce water-in-oil (w/o) Pickering emulsions when the surface of the nanocellulose is modified (Reviewed by Fujisawa *et al.*, 2017). An article of Costa *et al.* (2018) reported that cellulose nanofibers could be used as Pickering emulsifiers in o/w emulsions. The o/w emulsions were prepared by homogenizing 10 wt.-% sunflower oil and 90 wt.-% aqueous phase containing 0.01 wt.-% cellulose nanofibers. According to the authors the emulsions were prepared through pre-emulsification and subsequent double-stage homogenizer or an ultrasonication emulsification processes. The charge density of the cellulose nanofibers was reported to be an important parameter to control the kinetic stability of Pickering emulsions due to the electrostatic repulsion between the cellulose nanofibers. Zeta potential of the cellulose nanofibers was reported to decrease from initial -24.3 to -55.5 mV after using the high-pressure homogenizer with 70 MPa or ultrasound treatments with 675 W. This can be likely attributed that the high-pressure homogenizer and ultrasound probably promoted better agitation of the suspension and greater contact between cellulose nanofibers and oxygen, favoring the generation of negative charge on the surface of the cellulose nanofibers due to the partial oxidation of the particles. The preparation methods were also reported to have different effect on the stability of emulsions. The high-pressure homogenization was reported to cause coalescence phenomenon due to a less pronounced effect of shear stress on the cellulose nanofibers breakup and a reduced accommodation of cellulose nanofibers onto the oil droplet while the ultrasound caused enough particles to recover the oil droplets interface and prevented the coalescence phenomenon.

An article of Andresen and Stenius (2007) reported that surface modified MFC could be used to prepare water-in-toluene emulsions that have stability against coalescence and to increase the stability of emulsion against gravity induced sedimentation. They reported that MFC with varying hydrophobicity were prepared through surface silylation. The emulsion stability index (defined as the leveling-off ratio of the volume of the emulsified phase to the total volume, after storage in room temperature for five days) was reported to decrease when increasing the degree of surface substitution of MFC from 0.6 to 1.1, meaning that emulsion stability decreased with increasing hydrophobicity of the MFC. The droplet size was reported to be smallest for the degree of surface substitution of MFC of 0.6, which can be ascribed that the higher stability enabled from small droplet size would result in the decrease of the sedimentation velocity. When the authors compared the stability to sedimentation with increasing concentration of hydrophobic MFC, they noticed that the stability increased with increasing concentration of MFC, which was likely attributed to the increased viscosity of the continuous oil phase. The increase of the viscosity of the continuous phase could be caused by the interactions of the fibrils and microfibrils, which would promote the formation of three-dimensional MFC network in the continuous phase surrounding the drops and then reduced the extent of sedimentation.

A study of Beatrice *et al.* (2017) reported that cellulose nanofibers were used as composites with other polysaccharides to produce water-retaining foam for use as novel food structuring agents. Xylan was reported to act as a surfactant during mixing of the cellulose nanofibers and polysaccharides, which created a significant volume of air bubbles (40-60 %) in the suspension. The sizes of the bubbles were reported to range from tens to hundreds of micrometers. They also reported that the coarsening of foam due to merging bubbles was slowed down by the stabilizing polymers and cellulose nanofibers network.

2.2.2. Nanocellulose in food applications

For food applications, nanocellulose (cellulose nanofibrils, CNF) has been studied for ice cream formulation (Velásquez-Cock *et al.* 2019). They studied the influences of 0.15 and 0.3 wt % CNF from banana rachis on the structural elements of ice cream with two different fat concentrations. The studied structural elements included fat destabilization, melting rate, hardness, thermo-rheology, and ice crystal size. The authors reported that melting rate of ice cream with 10 wt % fat decreased to 0.43 ± 0.04, 0.28 ± 0.03 and 0.18 ± 0.03 g min^{-1} when the CNF concentration in the ice cream increased from 0 to 0.15 and to 0.30 wt %, respectively. The authors also reported that the ice cream reinforced by the cellulose nanofibrils was more creamy and smoother than the unreinforced ice cream, possibly due to the capability of CNF to initially reduce the melting sensation and improve the body of the ice cream. Another study (Sun *et al.*, 2015) reported the

effect of mixture of soybean protein isolate (SPI) and cellulose nanofiber on properties of ice cream. The authors replaced 10, 20 and 30 % cream in the ice cream by SPI-cellulose nanofiber mixture with ratio of 7:1, and found out that the melting rate of ice cream decreased from initial 51.38 to 21.98 % when the replacement of cream with SPI-cellulose nanofiber mixture increased from 0 to 30 %. There were no differences in textural profile analysis attributes of the ice cream except for adhesiveness, which decreased with increasing replacement of cream from 0 to 30 %.

An article of Golchoobi *et al.* (2016) studied the interactions between nanofibrillated cellulose, guar gum and carboxy methylated cellulose in low-fat mayonnaise (30 % lipids). The authors concluded that addition of nanofibrillated cellulose and guar gum to low-fat mayonnaise improved the physico-chemical, rheological and organoleptic characteristics of the product. Khorasani and Shojaosadati (2017) evaluated the effect of microencapsulation of the probiotic *Bacillus (B.) coagulans* using composites of pectin with nanochitin, nanolignocellulose and bacterial nanocellulose. They concluded that bionanocomposite formulated with 50 % pectin, 25 % nanochitin and 25 % nanolignocellulose was promising matrix for microencapsulation. The microencapsulation protected the probiotic cells in the low pH environment (pH 3.6 peach juice) over 5-week storage at 4 and 25 °C. Bacterial cellulose also increased the cooking loss and softening effects on the structure of Chinese-style meatballs (Lin and Lin, 2004) and enhanced the quality of bread, promoting higher specific volume, porosity, luminosity, moisture retention and tender crumb (Corral *et al.*, 2017). An article of DeLoid *et al.* (2018) reported the ability of ingested nanocellulose materials to reduce digestion and adsorption of ingested fats. Additionally, bacterial cellulose was reported to partially adsorb cholesterol-esters in solution and with some assurance of success to act as cholesterol binder in the mammalian digestive track (Stephens *et al.*, 1990).

2.2.2.1. Patent applications of nanocellulose for foods

An article of Gómez *et al.* (2016) reported applications of nanocellulose on various foods. For example, a patent of Turbak *et al.* (1982) reported the usage of MFC in food products. The invention stated that it was possible to prepare a wide variety of food products with MFC in a single stage operation in which the MFC is prepared *in situ*. The method converted the cellulose into MFC and produced a food product in the form of a homogeneous, stable suspension containing MFC. Food products included fillings, crushes, soups, gravies, puddings, dips, toppings, and other food products. The authors reported that the process of the invention comprised mixing the cellulose swelling edible liquid (water or edible lower alcohols such as ethyl alcohol, glycerine and propylene glycol), a food additive and fibrous cellulose to form a liquid suspension. The suspension was repeatedly passed through a small diameter orifice in which the mixture was subjected to a pressure drop of at least 3000 pounds per square inch gauge, a high velocity shear and a high

velocity decelerating impact. Another patent (Turbak *et al.*, 1983) reported the usage of MFC to increase the stability of the suspension. The authors reported that the MFC was prepared by repeatedly passing a liquid suspension of fibrous cellulose through a high pressure homogenizer until the suspension became stable. The MFC was prepared *in* situ in the suspension in a single stage operation by passing the liquid suspension through a small diameter orifice or alternatively by mixing the liquid which swells cellulose, the finely divided material suspended in the liquid and the separately prepared microfbirillated cellulose. The amount of MFC used in the preparing the suspensions were from about 0.25 % to about 5 %. One of the examples that the authors mentioned for MFC was the use as a substituent for oil to produce low calorie salad dressings. The other examples included the usage as an additional ingredient in sausage or hamburger. A patent of Innami and Yoshitaka (1987) reported the usage of MFC and water-soluble saccharide to produce a composition being effective in treating intestinal disorders. The composition was 15 wt.-% to 65 wt-% of MFC and 85 wt.-% to 35 wt.-% of water-soluble saccharide. The additional water-soluble saccharide was natural saccharide or water-soluble cellulose-derivative, such as sucrose, pectin, guar gum, mannan, xanthane gum, carboxymethylcellulose, sodium alginate, and hydroxymethylcellulose. A powdery composition could be prepared by adding the water-soluble saccharides to MFC suspended in water at a ratio of from 85/15 to 35/65 on solid basis, and then mixing them and drying. It was readily dispersed to give a stable aqueous suspension when added to water. The powdery composition was used as food additive in the form of paste or slurry by mixing it with water or taken separately as a drug when molded into tablets. A patent of Koh and Hayama (1997) reported the usage of MFC as an ingredient in emulsifier system to emulsify whipped cream. A patent of Cantiani *et al.* (2002) reported that dried CMF could be used in food formulations. They reported that it was known from practice that dried microfibrils were not redispersible in formulations due to the strong hydrogen bonds between the fibrils, and thus such additives were required in the drying. The subject of the invention was the use of combination of essentially amorphous cellulose CMF having a degree of crystallinity of less than or equal to 50 % with at least one polyhydroxylated compounds as an additive. The total amount was from 0 to 20 % of the total weight of the food formulation. They reported that the CMF have a cross section from approximately 2 to 10 nm. The microfibrils could be used as additives in formulations intended to be rendered in an overrun state (whipped creams, chantilly creams, toppings and ice-creams). Additionally, the combined microfibrils could similarly be used in compositions including mayonnaises, vegetable mousses, mousses comprising proteins, meat mousses, fish mousses and mousses comprising albumin. They reported also that the combined microfibrils had a capability to control and inhibit crystal growth. This was desired for foods that undergo temperature cycles (freezing, heating), such as ice cream and frozen foods as the formation of ice crystals would otherwise give the food an undesirable texture. Some other food applications of combined CMF included the replacement of animal gelatin. Also, the combined microfibrils were especially

good as stabilizers and thickeners of emulsions and/or dispersions of the formulations of vinaigrettes, additives in fruit juices, vegetable juices and milk-based drinks. The dried combined CMF were compatible with the milk-based media and reduced the sedimentation of the chocolate in chocolate-flavored milk-based drinks. According to the authors, the combined CMF could also modify the viscosity in yoghurts. A patent of Kleinschmidt *et al.* (1988) reported the usage of cellulosic fibrils and microfibrils in filling containing, dough-based products. The network of fibrils and microfibrils functioned as a flow control agent, which permitted the filling, and dough forming the crumb, to be co-baked. The surface of the fibrils usually had exposed microfibrils that were believed to cause fibrils to adhere together to form network. The authors indicated that the microfibrils were generally shorter than the fibrils and had a length of from approximately 1 to t 100 microns. The authors wrote that fibrils had a diameter of from about 0.1 to about 2 microns and the microfibrils had a diameter of from about 0.025 to about 0.1 microns. One of the claims was the flavored-filling which comprised an aqueous phase, dissolved sugar, network of cellulose fibrils and microfibrils dispersed in the aqueous phase, dissolved edible polyol humectant and selected from the group consisting of glycerol, sorbitol, propylene glycol and 1,3 butanediol and high methoxy pectin.

2.2.2.2. Nanocellulose and food safety

According to a study of He *et al.* (2019) novel nanomaterials have not been used in human food except titanium dioxide and iron oxide, which have been used as food pigment and colorant, respectively. The reason is that the regulation and the legislation is limited regarding nanofood, especially due to the complexity of nanomaterials and case-by-case legislating procedure. An article of Gómez *et al.* (2016) reported that nanocelluloses exhibit unknown properties and may expose human and the environment to unknown risks. The authors claimed that in nanomaterials, one could not evaluate the biological impacts merely on their chemical characteristics. For example, the size, shape, aggregation properties may affect the interactions of nanocelluloses with cells and other living organism. A study of Vartiainen *et al.* (2011) studied the health and environmental safety aspects of microfibrillated cellulose. The authors reported that the viability of mouse macrophages did not decrease after exposure to the friction ground microfibrillated cellulose for 24 hours exposure time. Neither inflammatory effect was shown on human monocyte derived macrophages, nor mouse macrophages after 6 hours exposure. A study of Endes *et al.* (2016) reported that 10 out of 19 various biological systems showed cytotoxicity response of nanocellulose. According to the article, the importance of relevant exposure system (cell type), dose, nanocellulose type/treatment/origin together with a clear material characterization was especially highlighted relating to the cytotoxicity of nanocellulose. As for inflammatory response,

the authors pointed out five out of seven references in which positive inflammatory response of nanocellulose occurred and two references in which negative inflammatory response was reported. Additionally, six out of nine references showed oxidative stress response caused by nanocellulose and three showed no oxidative stress response. For genotoxicity, the authors reported that four out of seven references, showed a genotoxicity response caused by nanocellulose and three references were it was not shown. The article finally stated that clarity must be obtained as to the health implications of low dose, chronic and repeated exposure to nanocellulose in its many different forms. Overall, the authors reported that the data seemed to suggest that under realistic doses and exposure scenarios, nanocellulose had limited associated toxic potential, even though certain forms of nanocelluloses could be associated with more hazardous biological behavior due to their specific physical characteristics.

2.3. Adsorption of phospholipids on nanocellulose

Nanocellulose has a hydrophilic surface due to the large amount of hydroxyl groups on the surface. Adsorption of phospholipids on the surface of nanocellulose is a potential method to increase the hydrophobicity of nanocellulose and to increase the compatibility of nanocellulose with vegetable oil. A study of Kostritskii *et al.* (2017) reported that there existed strong interaction between polar lipid head groups and the hydrophilic surface of crystalline cellulose. The authors identified two major types of interactions between palmitoyl-oleoyl-phosphatidyl choline (POPC) molecules and cellulose chains, including direct attractive interaction between lipid choline groups and oxygens of hydroxyl (hydroxymethyl) groups of cellulose, as well as the hydrogen bonding between phosphate groups of lipids hydroxymethyl/hydroxyl groups of cellulose. The authors reported that the water concentration at the phospholipid-cellulose interface decreased the interaction energy. At the highest water concentration (30 water molecules), the interaction energy was almost zero, which indicated the absence of lipid-cellulose interactions. For lower water concentrations (20, 10 and zero water molecules), the lipid-cellulose interactions were negative. The authors reported that the absolute interaction energy values became more attractive with dehydration. They divided the interaction energies into electrostatic (Coulomb) and Lennard-Jones components, and noticed that at lower water concentrations, the Coulomb interaction prevailed the interactions. The authors also reported that the hydrophobic lipid chains did not interact with a cellulose chain directly. They claimed that the only impact of support on hydrophobic acyl chains of lipids was dehydration of the lipid bilayer, which led to the decrease of the area per lipid and correspondingly to the enhanced ordering of lipid acyl chains. Kostritskii *et al.* (2017) observed that the chain ordering when the hydration decreased from 30 to 10 water molecules per lipid was not altered. The authors concluded that the exocyclic hydroxymethyl groups O6(O16) of cellulose showed better access to

choline and phosphate groups of phospholipids as compared to hydroxyl groups. In the meanwhile, at a very close juxtaposition between a lipid bilayer and a cellulose crystal, the contribution of the hydroxyl groups O2(O12) into the lipid/cellulose interactions became comparable with that of the hydroxymethyl groups O6(O16). Thus the chemical modification that inhibits the ability of the hydroxymethyl/hydroxyl groups of cellulose to form hydrogen bonds with lipids could weaken the adhesive interactions between cellulose-based materials and cell membranes.

Gurtovenko *et al.* (2018) reported that the phospholipid-cellulose binding was energetically favorable. They normalized the free energy by the number of dimers on the surface of cellulose crystal, and the free energy of binding of a cellulose dimer to POPC and palmitoyl-oleoyl-phosphatidyl ethanolamine (POPE) lipid bilayers were estimated to be -1.89 ± 0.03 and -1.96 ± 0.03 kJ/mol, respectively. They reported that the binding of cellulose had a strong effect on the structure of the lipid bilayer that resulted in a pronounced asymmetry in the density profiles of the opposite bilayer leaflets. The distal leaflet was reported to be largely unaffected by the binding of cellulose and the proximal leaflet that was next to the cellulose crystal surface underwent considerable structural changes. They also reported that the interactions of the O6(O16) oxygen atom of the exocyclic hydroxymethyl groups of cellulose chains with lipid head groups could be stronger compared to the oxygen atoms O2(O12) and O3(O13) of the hydroxyl groups of cellulose chains. They reported that the phosphate groups of POPE lipids established larger number of hydrogen bonds with the cellulose than POPC lipids. This result can likely be attributed to the smaller size of NH_3-groups of the POPE lipid head groups than the choline groups of the POPC lipids, so that the NH_3-groups of the POPE lipid head groups hindered the access to the phosphate groups to a lesser extent compared to the POPC lipids. As a result, the cellulose hydroxyl groups came closer to the POPE phosphate groups. They also reported that the POPE head groups were capable of hydrogen bonding with other lipids in the monolayer which made it more horizontally oriented with respect to the bilayer surface, promoting the contact between cellulose and POPE phosphate groups. The NH_3-groups of the POPE lipids could also serve as donors of hydrogen bonds between POPE lipids and oxygen atoms of hydroxyl (hydroxymethyl) groups of cellulose, which was reported to be absent in the POPC-cellulose system. They reported that a positive increase in the energy due to dehydration of the interfacial region for the POPE-cellulose system exceeded that for the POPC counterpart, and an excess in the number of formed POPE-cellulose hydrogen bonds was balanced by the breakage of POPE-water and cellulose-water hydrogen bonds, which led to the similar values in the free energy of binding for both POPC and POPE lipid bilayers.

An article of Zhang *et al.* (2015) reported that lecithin could be immobilized on bacterial cellulose nanofibers *via* immersing into alcohol solutions of lecithin. The immobilization of lecithin by treating the bacterial cellulose pellicles in alcohol was studied at various lecithin concentrations, and the lecithin was cross-linked with proanthocyanidin. Without crosslinking, the morphological differences of the fibers with lecithin were hardly observed in scanning electron microscope (SEM) at lower lecithin concentrations in the alcohol solution, however, the adsorbed lecithin was indeed identified at higher lecithin concentration. With cross-linked lecithin, lecithin spheres were observed on the surface of bacterial cellulose. It has been found that bacterial cellulose nanofibers were wrapped with continuous lecithin layer at 2.0 wt.-% lecithin concentration with cross-linking. They also reported that the contact angle of bacterial cellulose increased with increasing lecithin concentration in the treatment solution from 50.0° for bacterial cellulose to 70.0° after treating with 2.0 wt.-% lecithin in alcohol.

3. Experimental

The experimental section consists of two parts: first, the summary of the published paper in which the effect of different control parameters on the reverse micelle formation of phospholipids in vegetable oil were studied; second, the supplementary experiments of the surface modification of nanocellulose. The aim of the supplementary experiments is to attach the phospholipid structures onto nanocellulose. Later, we may use phospholipid-nanocellulose materials as structuring agent or filler in vegetable oil. From now on in the thesis, the word lecithin is used to refer the phospholipid material used in the laboratory experiments and the word phospholipid is used to refer phospholipids generally.

3.1. Summary of the publication

The publication describes the influence of temperature, water concentration and free fatty acid on the aggregation of phospholipids and free fatty acids in vegetable oil. This is especially important for the vegetable oil purification process called degumming in which water is used to remove phospholipids and other surface-active components from the oil. Very few investigations had used vegetable oil as the nonpolar media when studying the phospholipid reverse micelles in organic solvents. The examined parameters affected the self-assembly of the phospholipids in oil, but the most remarkable effect was the combined effect of free fatty acids and water. The publication leads to a better understanding to control the self-assembly of phospholipids in vegetable oils systems. The influence of different parameters including, temperature, water and free fatty acids on the phospholipid aggregation in rapeseed oil was studied using the 7,7,8,8–tetracyanoquinodimethane

dye (TCNQ) solubilization method. The principle of the TCNQ solubilization method is that the reverse micelles solubilize the TCNQ, which can lead to a sharp rise in absorbance around *cmc*. The shape of the lecithin aggregates were investigated using SAXS and cryogenic transmission electron microscopy (Cryo-TEM). Molecular simulations were performed to further investigate the influence of oleic acid on the reverse micelle formation of lecithin in rapeseed oil.

Results showed that phospholipids acted as surface-active molecules in oil and they formed reverse cylindrical micelles above *cmc* in the oil with small amount of moisture (~0.03 wt.-%). Increasing temperature from room temperature to 70 °C decreased the *cmc* of lecithin in vegetable oil at low water concentrations. No conformational changes of lecithin in rapeseed oil occurred between 10 to 90°C according to differential scanning calorimeter and thus it can be concluded that conformational changes had an insignificant effect on the aggregation of lecithin between room temperature and at 70 °C. In agreement with our findings, an article of Cui *et al.* (2014) reported that the *cmc* of 1,2-dioleoyl-sn-glycero-3-phosphocholine and 1,2-dioleoyl-sn-glycero-3-phosphoethanolamine in soybean oil decreased with increasing temperature. Effect of free fatty acids on the aggregation of lecithin reverse micelles in rapeseed oil was studied by adding different concentrations of oleic acid into the system. Oleic acid itself did not form reverse micelles in rapeseed oil with 0.3 wt.-% added water at any of the studied concentration (0.03-80 wt.-%) at room temperature. The *cmc* of lecithin was determined in rapeseed oil with different oleic acid concentrations. The *cmc* of lecithin increased from 0.055 wt.-% to 0.20 wt.-% at 70 °C when oleic acid concentration of the system increased from 0 wt.-% to 20 wt.-%. At a concentration of oleic acid above 20 wt.-%, the *cmc* could not be detected below 3 wt.-% lecithin and higher concentration of lecithin could not be solubilized in the oil. The *cmc* of lecithin also seemed to increase with increasing oleic acid at room temperature. However, the *cmc* of lecithin could be determined only at oleic acid concentration from 0 wt.-% to 10 wt.-% as at higher oleic acid concentration, the *cmc* of lecithin was above 3 wt.-% that was more than could be solubilized into oil.

Small amounts of water hydrated lecithin cylindrical reverse micelles into lamellar crystalline structures. The lamellar structures precipitated from the vegetable oil. The precipitation of lecithin was observed to occur with small addition of water and the removal of solubilized lecithin aggregates was indicated by the decrease in absorbance as shown in Figure 4A. The precipitation was seen clearly already at water-to-lecithin ratio 13.7 wt.-% at room temperature (Fig. 4B) and 20.9 wt.-% at 70 °C (Fig. 4C). As seen from Figure 4A, the lowest absorbance was at water-to-lecithin ratio of 43.2 wt.-%. After the lowest absorbance value, the precipitate reached the water saturation point (indicated as “X” in the Fig. 4A). At higher water-to-lecithin weight ratio (52.7 wt.-%), the sample became turbid, due to the formation of small water droplets in the supernatant

phase. At 70 °C, the absorbance values were not in the spectrophotometer absorbance limit (<1) as the reaction between the lecithin and the fluorescence dye TCNQ led to very dark colors (Fig. 4C). The absorbance data that was above value 1 is not shown because it does not represent the true quantity for absorbance. However, the precipitation of lecithin aggregates was observed at the water-to-lecithin weight ratio of 20.9 wt.-% at 70 °C as indicated by the photograph of the samples in Fig. 4C. Thus, it could be concluded that the trend at elevated temperatures was qualitatively similar to the response at room temperature. The maximal water adsorption capacity of lamellar crystalline structures was at water-to-lecithin weight ratio of 43.2 to 103.6 wt.-% and 121.9 to 140.1 wt.-% at room temperature and 70 °C, respectively. In excess water above the water saturation concentration of the lecithin precipitate, water droplets appeared into the oil and caused turbidity. In close agreement with our measurements, previous studies had reported that excess water phase separates above 34-47 wt.-% (water-to-lecithin) in various solvents (Lei *et al.*, 2003 and Angelico *et al.*, 2000).

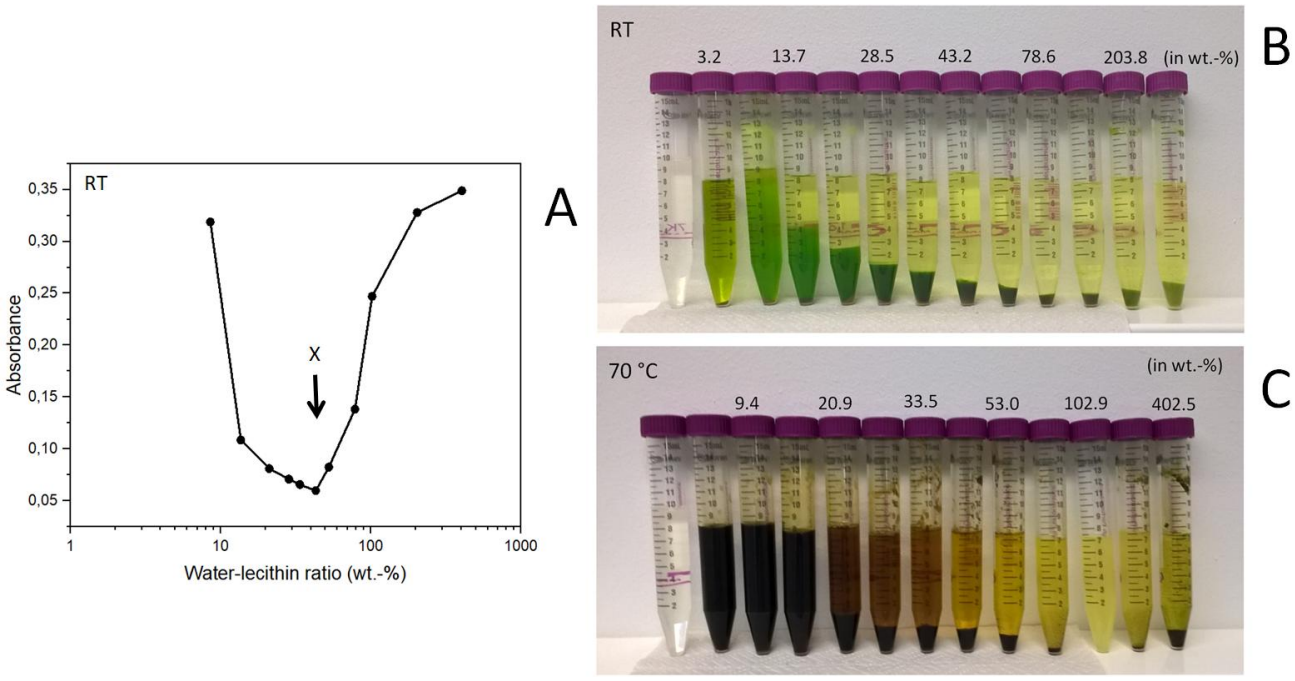

Figure 4. Absorbance using TCNQ-dye as a function of water-lecithin weight ratio (wt.-%) in rapeseed oil with 1 wt.-% lecithin at room temperature (RT) (A). X refers to the water saturation point. A photograph of the sample tubes at room temperature (B) and sample tubes at 70 °C (C). The numbers above the sample tubes in B and C corresponds to water-to-lecithin weight ratio (wt.-%). (Lehtinen *et al.*, 2017)

The morphology and structure of lecithin aggregates, in other words reverse micelles and precipitate, were further studied using small-angle SAXS measurements and cryogenic Transmission electron microscopy (cryo-TEM) imaging at room temperature. Cryo-TEM and SAXS

analyses of the solubilized sample (corresponding to the second sample tube from the left in Fig. 4B but without the TCNQ dye) are shown in Figure 5. According to the SAXS pattern, the sample is amorphous (non-crystalline) (Fig. 5B). In the cryo-TEM image (Fig. 5A), some of the lecithin micelles were perpendicular to the plane of the image and hexagonally packed according to the Fast Fourier Transform (FFT). This indicated that the lecithin reverse micelles had long narrow shape and the structures were cylindrical rather than spherical.

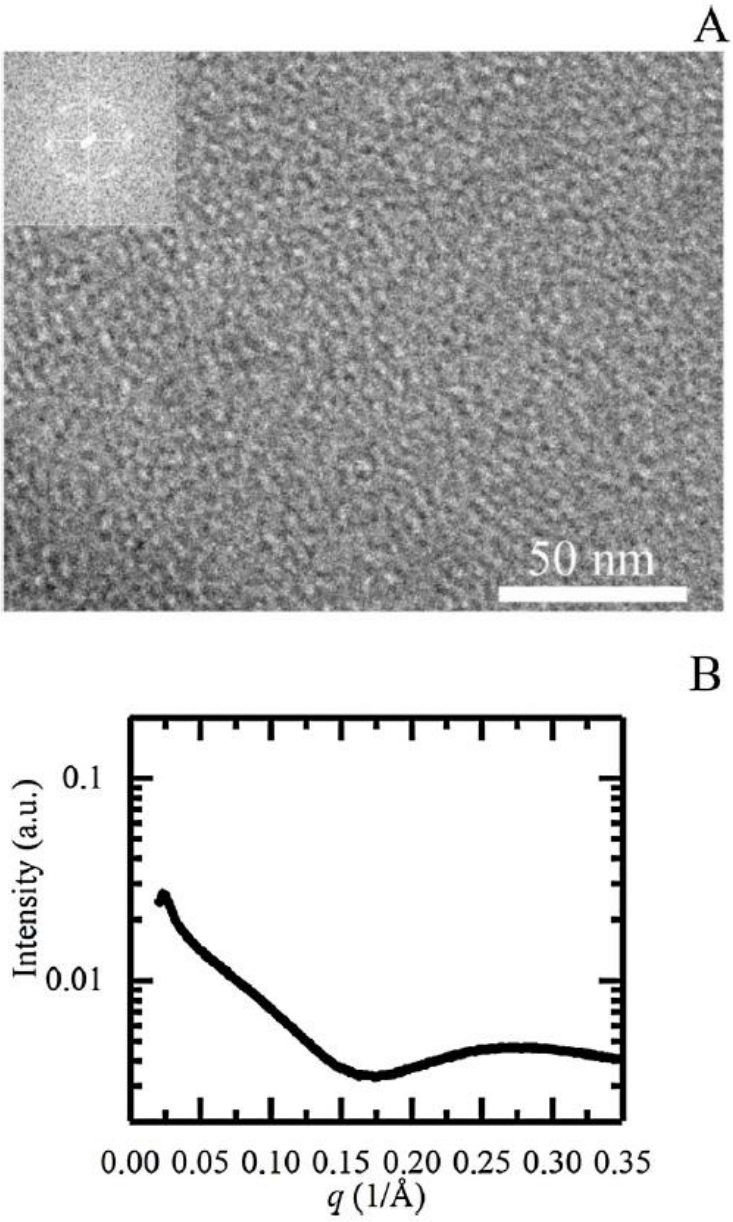

Figure 5. Cryo-TEM images (A) and SAXS patterns (B) of the 1 wt.-% lecithin in rapeseed oil containing 0.03 wt.-% water at room temperature (Inset figure: Fast Fourier Transform (FFT) of cylindrically packed structure). (Lehtinen *et al.*, 2017)

Analysis of the sample of 1 wt.-% lecithin in rapeseed oil with water 0.21 wt.-% at room temperature showed two phase system: the upper supernatant phase and the lower precipitate phase (Figure 6). The sample corresponds to the fifth sample tube from the left in Fig. 4B but without the TCNQ dye. According to the SAXS measurement, there was a crystalline phase present in the upper phase indicating a presence of lamellar structures (Fig. 6B). The SAXS measurement of the lower phase revealed that there were lamellar structures present with higher intensity than in the upper phase indicating that the lamellar structures were concentrated in the lower phase (Fig. 6A). The Bragg peaks of the lamellar structures at 1:2 relative positions lead to a distance between the lamellar planes of 5.03 nm ($d = 2\pi/q$) according to SAXS. The cryo-TEM image of the precipitate phase confirmed that the structures were lamellar (Fig. 6A), with a distance between the layers of approximately 5 nm according to the FFT. A possible explanation for the formation of lecithin lamellar liquid crystalline structures with addition of water was that the adsorption of water increased the volume of phospholipid-head groups in lecithin which had an effect on the packing parameter of the phospholipid molecules at the water-oil interface. With swollen head groups, the lecithin could not maintain the reverse cylindrical shape that was soluble to oil due to the energetically unfavorable packing and they were forced to form lamellar liquid crystal structures with lower interfacial curvature and lower solubility in rapeseed oil.

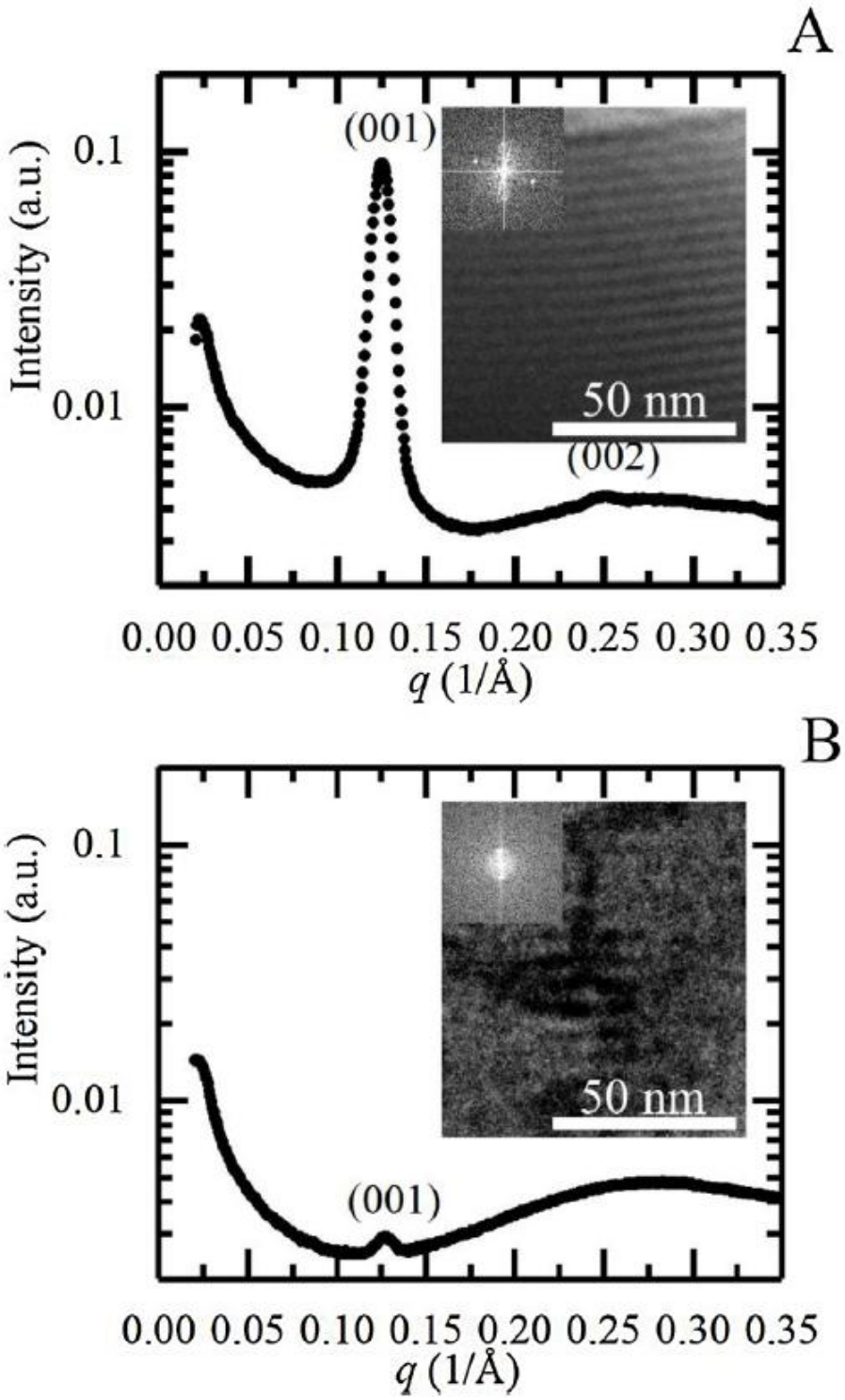

Figure. 6. SAXS patterns of (A) the lower precipitated phase and (B) the upper soluble phase of 1 wt.-% lecithin in rapeseed oil at room temperature at water-to-oil weight ratio of 0.21 wt.-%. Inset figures: cryo-TEM and Fast Fourier Transform (FFT). (Lehtinen *et al.*, 2017)

The influence of water concentration on lecithin in rapeseed oil with varying oleic acid concentrations is shown in Figure 7 at room temperature and at 70°C. Lecithin concentrations that

were studied were 1 wt.-% at room temperature and 0.2 wt.-% at 70 °C both concentrations which contained abundantly lecithin reverse micelles without addition of water or oleic acid (Fig. 7A and 7C). According to TNCQ experiments, oleic acid in rapeseed oil increased the solubility of lecithin into the oil, and suppressed the formation of lecithin reverse micelles at low water content at room temperature. In presence of more water, oleic acid stabilized the reverse micelles and consequently more water was needed to induce the phase separation (Fig. 7A). Lower lecithin concentration (0.2 wt.-%) at 70 °C was chosen due to the reaction of lecithin reverse micelles with TCNQ at higher temperature that lead to very dark colors with 1 wt.-% lecithin concentration and almost all the experimental points had absorbance above 1 that was above the correct measurement range for spectrophotometer. In Fig. 7A, the absorbance of the lecithin reverse micelles decreased with increasing oleic acid concentration when there was only a trace amount of water (water-to-lecithin ratio 3.2-3.6 wt.-%) that originated from the materials. The decrease in absorbance with increasing oleic acid concentration correlated with the trend discovered in the *cmc* experiments of lecithin in rapeseed oil with increasing oleic acid concentrations. With absence of oleic acid, the addition of small amount of water (water-to-lecithin ratio approximately 8.6 wt.-%) caused a significant decrease in absorbance indicating the removal of solubilized reverse micelles from the oil. In Fig. 7A, the dashed lines were used to mark the absorbance above 1 that was beyond the reliable measurement range of the spectrophotometer and the absorbance values above 1 can be used only as indicative data points. The absorbance was much more stable in systems containing oleic acid when increasing the water-to-lecithin ratio (wt.-%). In presence of 5 wt.-%, 10 wt.-% and 20 wt.-% oleic acid the water-to-lecithin weight ratio required to induce the decrease in absorbance was above approximately 14 wt.-%. This indicated that a moderate amount of oleic acid enhanced the solubility of lecithin into the oil and thus more water is required for the lamellar structures to be formed. The Fig. 7B shows the water saturation points of lecithin at various oleic acid concentration. The water saturation point of lecithin was the concentration of water at which the turbidity of the system started to increase causing an increase of absorbance. The water saturation range of lecithin is seen in a range of water-to-lecithin weight ratios between 43.2 wt.-% and 103.6 wt.-% depending on the oleic acid concentration. Above water saturation concentration, lecithin became fully hydrated and water droplets were formed into the oil in all measured oleic acid concentrations which was seen as increase in absorbance. Somewhat similar trends were observed when adding water into rapeseed oil that contained lecithin (0.2 wt.-%) at 70 °C. The measurement points above the absorbance value 1 are also shown but they should be used only as a qualitative indication of the presence of lecithin reverse micelles. At 70 °C (Fig. 7C, an increasing oleic acid concentration decreased the amount of initial lecithin aggregates and the water saturation point was between water-lecithin ratios 121.9 wt.-% to 140.1 wt.-% depending on the oleic acid concentration. Above the water saturation point, water droplets appeared into rapeseed oil causing turbidity and a rapid increase in absorbance. In contrast to systems at room

temperature, moderate oleic acid concentrations at 70°C did not seem to have peculiar effect on aggregation of lecithin and the amount of lecithin aggregates decreased independently from water concentration in all systems with oleic acid. The exception was the system with no oleic acid in which the suppression of the lecithin reverse micelles was clearer and the decrease of absorbance started above water-lecithin ratio 41.1 wt.-%. Thus, it could be concluded that moderate amounts of oleic acid in the oil (5, 10 and 20 wt.-%) could delay the removal of lecithin reverse micelles upon addition of water, and the formation of lamellar structures required more water. According to the molecular simulations, the oleic acid bound dominantly to the phosphate group and formed a shell around the lipid head group. Water molecules could hydrogen bond with the oleic acid molecules already bonded with the lipid head group. This leads to the enhanced solubilization of phospholipid in vegetable oil in accordance with the experimental data.

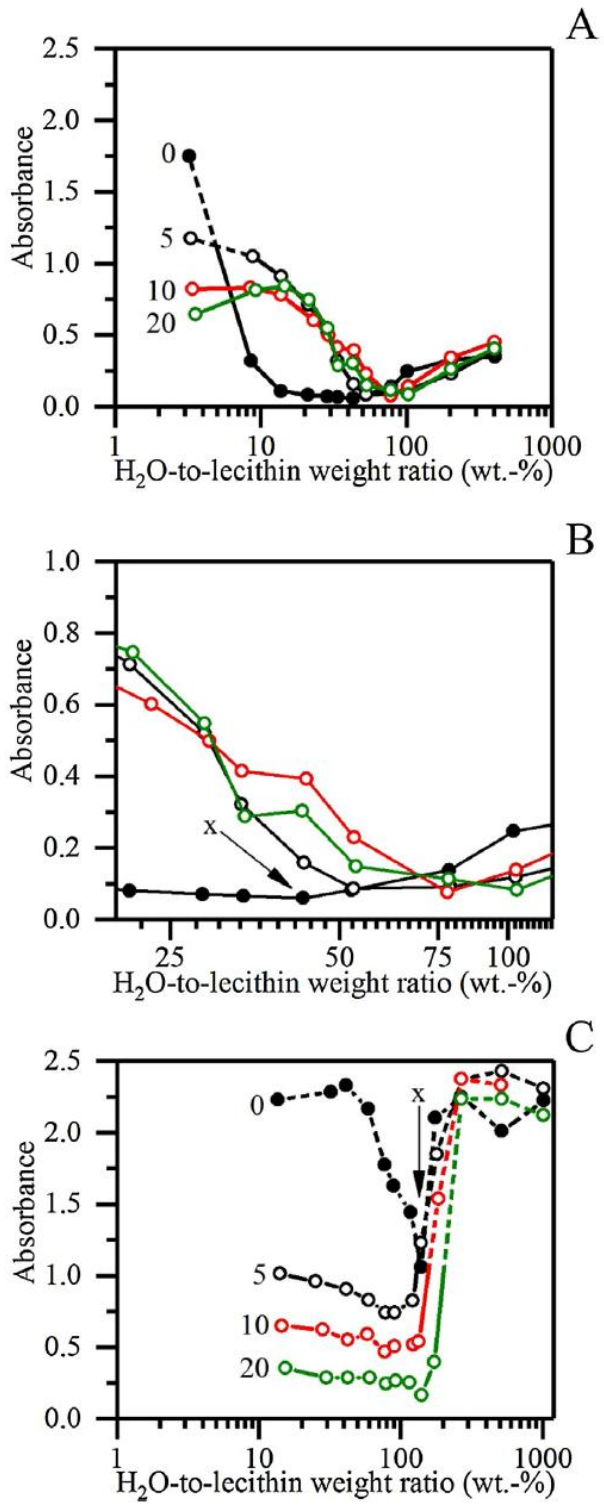

Figure 7. TCNQ absorbance as a function of water-to-lecithin weight ratio (wt.-%) in rapeseed oil containing (A) 1 wt.-% of lecithin at room temperature, (B) a zoom in on the system at room temperature and (C) 0.2 wt.-% of lecithin at 70◦C. UV absorbance values >1 are shown for qualitative comparison as dashed lines. X refers to the water saturation point for the system without added oleic acid. (Lehtinen *et al.*, 2017)

3.2. Supplementary experiments

The supplementary experiments were conducted in Aalto University, Espoo, Finland. The experiments involved the preparation of lecithin structures in vegetable oil and the surface treatment of cellulose nanofibrils (CNF) using the lecithin structures.

3.2.1. Materials and methods

3.2.1.1. Materials

Food-grade rapeseed oil (Keiju rypsiöljy, Bunge Finland Oy, Raisio, Finland) was purchased from a local super market. Granular L-Alpha-Lecithin, extracted from soybean oil, was purchased from Acros Organics (New Jersey, USA). The composition of lecithin was approximately 23 wt.% phosphatidylcholine, 20 wt.% phosphatidylethanolamine, 14 wt.-% phosphatidylinositol, 8 wt.-% phosphatidic acid, 8 wt.-% minor phospholipids, 8 wt.% sugars, 15 wt.% glycolipids, 3 wt.% triglycerides and 1 wt.% moisture. Cellulose nanofibrils were from Aalto University (Espoo, Finland). CNF was prepared by disintegrating never-dried, fully bleached and fines-free sulfite hardwood (birch) fibers obtained from a Finnish pulp mill, as described previously (Bai *et al.*, 2018). The fibers were disintegrated through a high-pressure microfluidizer (M110P, Microfluidics Int. Co., Newton, MA) using 6 passes. No chemical or enzymatic pretreatment was used prior to microfluidization. The average width of CNF was ~20 ± 8 nm, as shown in a recent study (Huan *et al.*, 2019). The dry mass concentration of the CNF was 2.0 wt.-%. The silica substrates were prepared from WaferShipper™ by scratching and fractionating it to pieces showing approximately one centimeter height and approximately one centimeter width. Poly(ethyleneimine) (PEI) solution was purchased from Sigma-Aldrich (St. Louis, Missouri, USA) and was diluted to 0.25 wt.-% concentration prior to use. Millipore water was purified using a Synergy UV water purification systems (Millipore SAS, Molsheim, France).

3.2.1.2. Preparation of lecithin lamellar structures

The lipid materials including rapeseed oil and lecithin were dried prior to solubilization. A stock solution of lecithin (2 wt.-%) in rapeseed oil was obtained by stirring the lipids and increasing the temperature from room temperature to 70 °C in 1 hour and then the temperature was kept constant for 2 h at 70 °C. The stock solution of lecithin was diluted using rapeseed oil to obtain solution of 1 wt.-% lecithin in oil. Then the solution was precipitated by adding 0.175 wt.-% Millipore water and

rotating it at room temperature for 2 h. After the precipitation the oil became turbid. The oil was stored at 6 °C overnight until the lecithin precipitate (LP) was observed at the bottom. The lecithin precipitate was centrifuged at 800 g for 20 min, and both supernatant and the precipitate were collected. The lecithin precipitate was diluted by adding 125.0 g of oil supernatant into 124.3 g of lecithin precipitate to obtain sufficient volume for the Langmuir-Blodgett (LB)-deposition trough.

3.2.1.3. Preparation of CNF-lecithin films

The interaction of lecithin with CNF was studied by preparing lecithin-CNF thin films on silica substrate. First, CNF solution was diluted to 0.12 % based on dry mass content using deionized water. The CNF suspension was then dispersed using an ultrasonication tip (Branson sonifier S-450 D) at 25 % amplitude for 1 min. Next, the CNF solution was centrifuged at 8000 relative centrifugal force (rcf) for 30 min at 20 °C, and the supernatant was collected for further use. Then the silica substrates were covered with cationic PEI solution settled for 10 min before rinsing with deionized water. Two types of substrate were prepared for CNF spin-coating: substrates with no pressurized air treatment leaving varying amounts of rinsing water on the PEI surface (type 1) and substrates with pressurized air treatment leaving no rinsing water on the PEI surface (type 2). The aim is to study the effect of dilution of CNF on the adsorption so that the air blowing step may be dismissed in the future experiments. Then drops of CNF were placed onto the substrates and the substrates were spin-coated (Laurell spin-coater WS-650SX-6NPP-Lite) at 4000 rpm for 1 min. After spin-coating, the substrates were stored under controlled humidity (~50 %). Then the substrate surfaces were dipped into the diluted lecithin precipitate using LB-trough. The contact time of the substrate surface with the diluted lecithin precipitate in the LB-trough was approximately 30 s after which the substrates were stored under controlled humidity (~50 %). After this, the substrates were rinsed with chloroform or ethanol to remove the lecithin precipitate. Due to the slight loss of lecithin precipitate during the LB-trough depositions, the lecithin precipitate was slightly diluted for the second and third repeats using the oil supernatant to obtain sufficient volume to fill the LB-trough.

3.2.1.4. Measurement of contact angle

The hydrophobicity/hydrophilicity of the substrates was characterized by the contact angle measurement. The contact angle of drops of water deposited on the substrates were measured using CAM 200 device (KSV Instruments). The used droplet was water, so higher contact angle indicated that the surface was hydrophobic and low contact angle value that the surface was hydrophilic.

3.2.1.5. Optical microscopy of vegetable oils

The vegetable oil samples were studied using an optical microscope. The samples included rapeseed oil and 2 wt.-% lecithin in rapeseed oil. Additionally, lecithin precipitate that was already used in LB-trough depositions, the oil supernatant and the lecithin precipitate that was used in LB-trough depositions with centrifuged again at 800 g for 20 min were imaged. Also, the supernatant of the second centrifugation was imaged.

3.2.2. Results and discussion

3.2.2.1. Yield of lecithin precipitate

The composition for current system is 98.825 wt.-% rapeseed oil, 1.000 wt.-% lecithin and 0.175 wt.-% added water. The total mass is 1320.11 g after three subsequent centrifugations. A centrifuged sample is shown in Figure 8. The yield of oil supernatant and lecithin precipitate was 1161.39 g and 130.94 g, respectively, and the loss of material was 27.78 g.

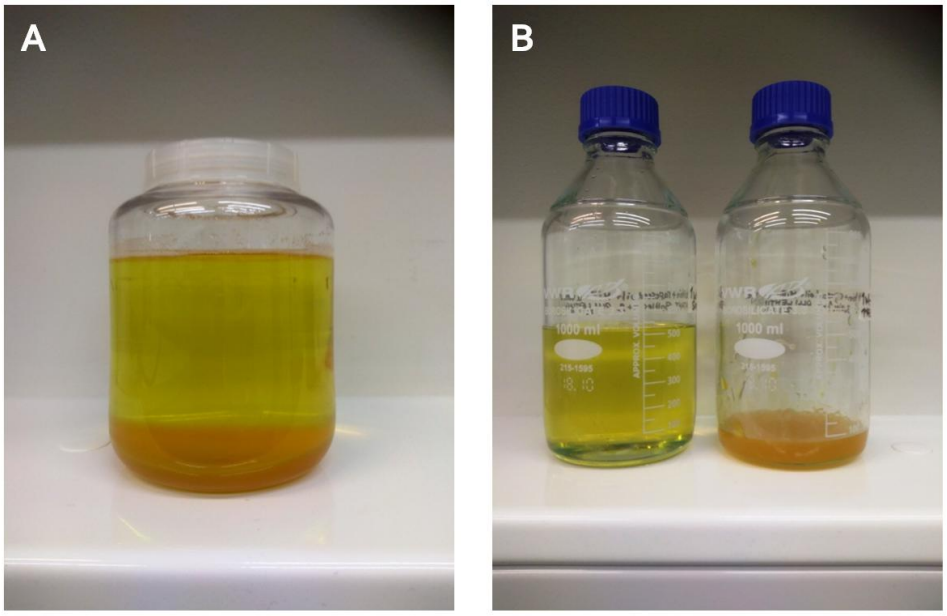

Figure 8. (A) Centrifuged rapeseed oil, lecithin, water mixture, and (B) oil supernatant (left bottle) and lecithin precipitate (right bottle) separated after centrifugation. The system composition was 1.000 wt.-% lecithin, 98.825 wt.-% rapeseed oil and 0.175 wt.-% added water.

3.2.2.2. Optical microscopy imaging

The aim of the optical microscopy was to evaluate the solubilization of lecithin into rapeseed oil and to investigate the morphology of the lecithin precipitate. Figure 9 shows the vegetable oil samples for optical microscopy imaging. By visual observation rapeseed oil (sample A), 2 wt.-% lecithin in rapeseed oil (sample B), oil supernatant (sample D) and oil supernatant from additional centrifugation of lecithin precipitate (sample F) were transparent. Lecithin precipitate diluted with oil supernatant (sample C) was turbid. Lecithin precipitate diluted with oil supernatant and being treated with additional centrifugation (sample E) was turbid and semi-solid.

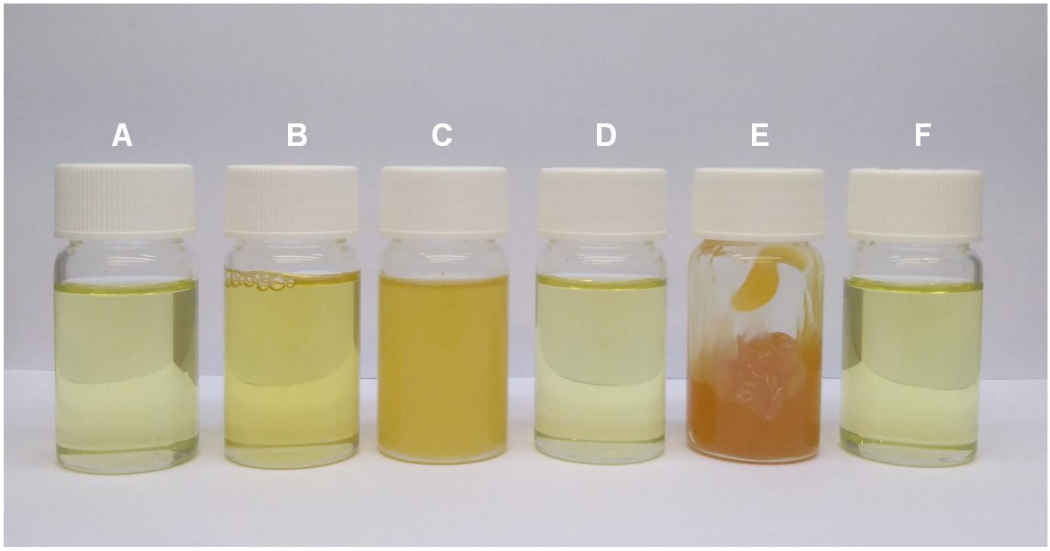

Figure 9. Vegetable oil samples for light microscopy imaging: (A) rapeseed oil, (B) 2 wt.-% lecithin in rapeseed oil, (C) lecithin precipitate diluted with oil supernatant, (D) oil supernatant, (E) lecithin precipitate diluted with oil supernatant and being treated with additional centrifugation, (F) oil supernatant from the additional centrifugation of lecithin precipitate.

Figure 10 shows the optical microscopy images of vegetable oil the samples. The sample of rapeseed oil (Fig.10A) showed no aggregates and very few particles. The sample of 2 wt.-% lecithin in rapeseed oil (Fig. 10B) showed very few tiny particles. This was an indication that lecithin was solubilized into the rapeseed oil. The sample of oil supernatant (Fig. 10D) showed some scattered particles. The sample of oil supernatant from additional centrifugation (Fig. 10F) showed few scattered particles. In the sample of lecithin precipitate that was diluted with oil supernatant (Fig. 10C), there were dispersed aggregates present that had diameters mostly above 50 µm. The edges and surfaces of the aggregates appeared to be uneven. There were longer appendages seen on some of the aggregates. The sample of lecithin precipitate with additional centrifugation (Fig. 10E), showed an image of full of grainy shapes. This indicated that the aggregate density was increased compared to diluted lecithin precipitate (Fig. 10C).

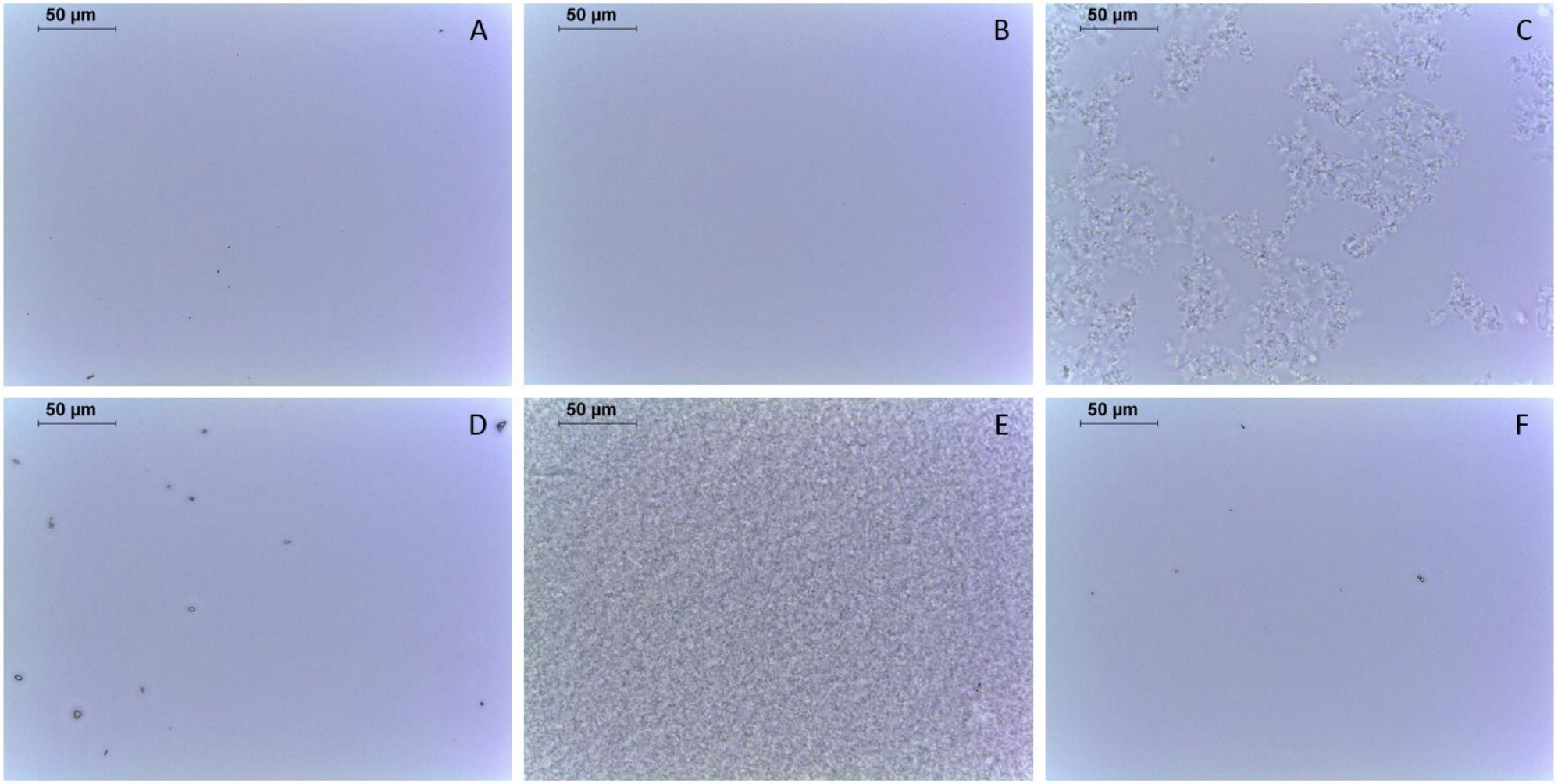

Figure 10. Optical microscopy images of vegetable oil samples: (A) rapeseed oil, (B) 2 wt.-% lecithin in rapeseed oil, (C) lecithin precipitate diluted with oil supernatant, (D) oil supernatant, (E) lecithin precipitate diluted with oil supernatant and being treated with additional centrifugation, (F) oil supernatant from additional centrifugation of lecithin precipitate.

3.2.2.3. Contact angle measurement

The lecithin precipitate could be potentially be adsorbed onto the surface of CNF and to form phospholipid bilayer (Figure 11). The purpose of the solvent rinsing was to investigate whether the adsorption of lecithin would be strong enough to sustain the rinsing, and thus giving an indication of the strength of the physical bond between CNF and phospholipids.

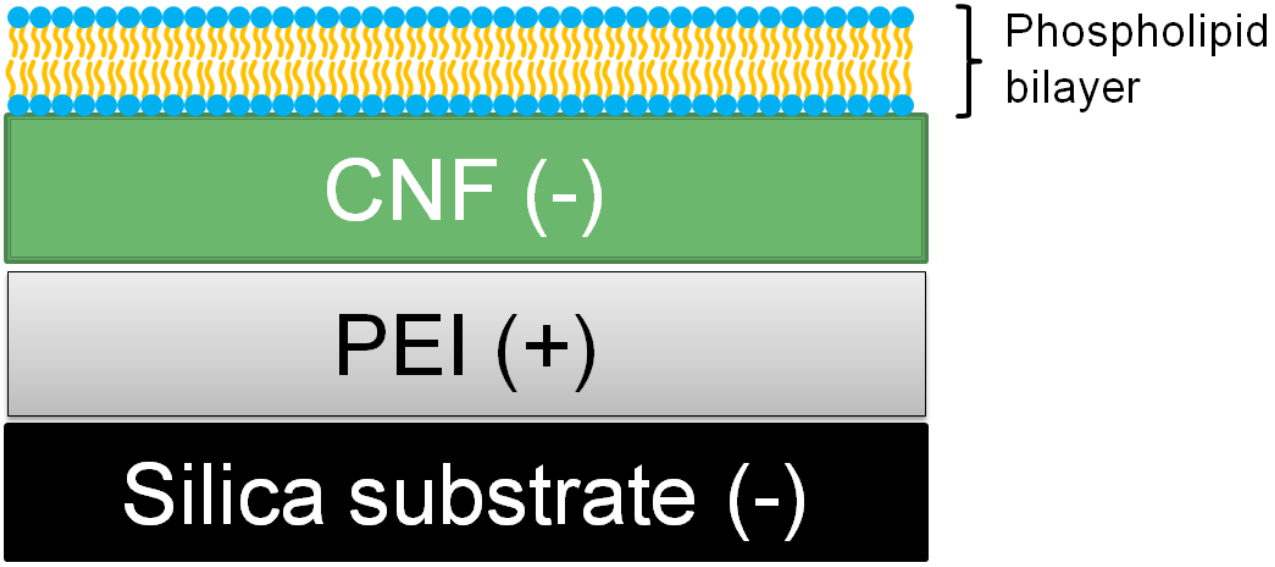

Figure 11. Illustration of the adsorption of different material layers on to the silica substrate in the experiments. PEI = poly(ethyleneimine), CNF = cellulose nanofibril. The surface charge of the material is shown in brackets.

Figures 12 and 13 show the first CA measurement round of substrates with different chemical treatments of type 1 and type 2, respectively. In Figures 12 and 13, the same substrate with no chemicals (CA value of 25.8 °) was used as a reference. This was suitable as the reference substrate was not treated with PEI solution that would be rinsed off and then air blown or not-air blown deciding whether it would be included to either type 1 or type 2.

In Figure 12, CA of the substrate treated with PEI+CNF+LP+ethanol 5 mL was 35.9 °. Compared to the CA of the substrate treated with no chemicals, the increase of CA value indicated that the addition of PEI+CNF+LP+ethanol 5 mL decreased the hydrophilicity of the surface as a water droplet did not wet the surface. When comparing the CA of the substrates treated with PEI+CNF+LP+chloroform 1 mL from the murky side (19.5 °) and PEI+CNF+LP+chloroform 1 mL from the clear side (34.1 °) to the PEI+CNF+LP+ethanol 5 mL (CA value of 35.9 °), it seemed that the rinsing with chloroform increased the hydrophilicity of the surface compared to ethanol rinsing.

It is not clear why the murky side would have increased the hydrophobicity as the murkiness was believed to be caused by the insufficient rinsing effect, which left thicker layer of lecithin precipitate onto the surface that would decrease the hydrophilicity. The highest CA of 39.9 ° was measured for the substrate treated with PEI+CNF+LP+chloroform 5 mL, indicating that 5 mL chloroform rinsing would be the most efficient in increasing the hydrophobicity of the surface. The visual appearances of sample surfaces treated with PEI+CNF+LP+chloroform 5 mL were clear, indicating that the rinsing removed excess lecithin precipitate.

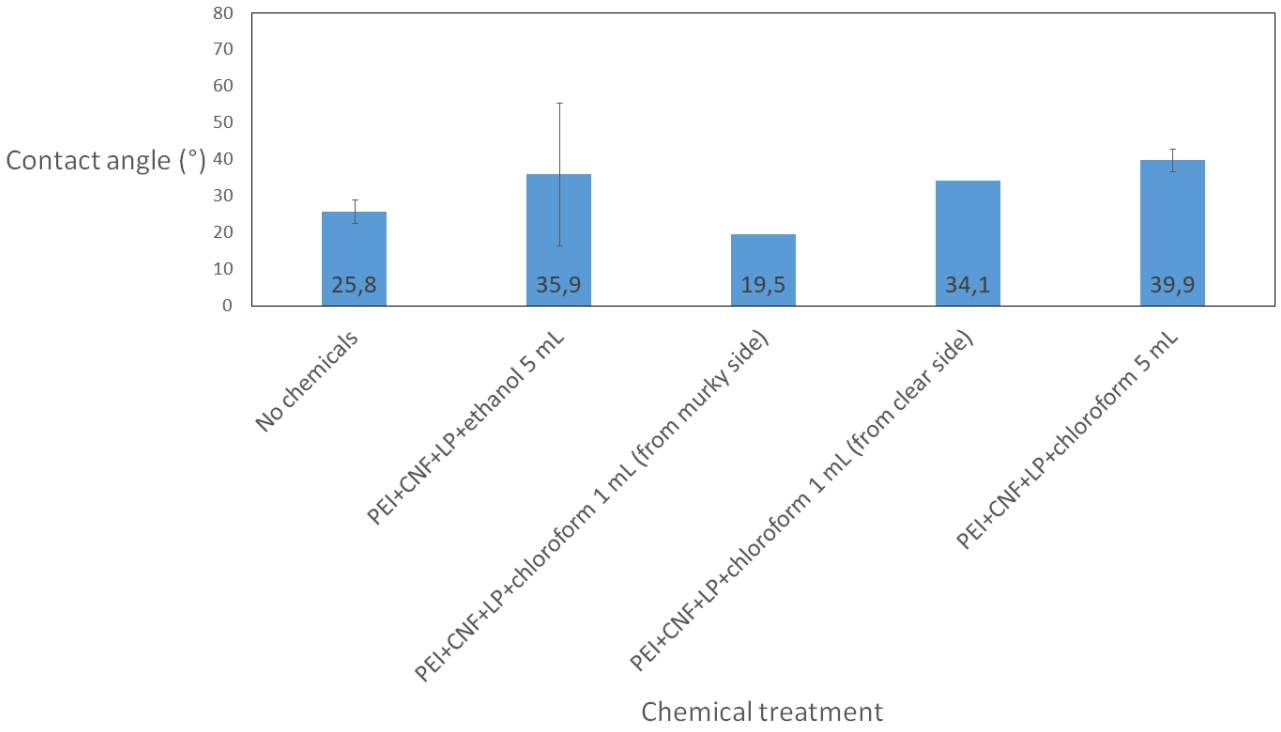

Figure 12. Contact angles of water on the substrates in the first measurement round of type 1. PEI = poly(ethyleneimine), CNF = cellulose nanofibrils and LP = lecithin precipitate.

In Figure 13, the CA of substrate with no chemicals was 25.8 ° and the CA of substrate treated with PEI+CNF was 19.3 °, which indicated that treating the surface with PEI+CNF increased the hydrophilicity of the surface as the wetting was improved. The CA of the substrate with PEI+CNF+LP+ethanol 5 mL was 28.4 °. This indicated that LP+ethanol 5 mL decreased the hydrophilicity of the substrate compared to the substrate treated with PEI+CNF. In the case of substrate treated with PEI+CNF+LP+chloroform 1 mL and PEI+CNF+LP+chloroform 5 mL, the CA was 23.2 ° and 27.3 °, respectively, which indicated that in both cases the hydrophilicity decreased compared to the substrate treated with PEI+CNF. This also means that the mixture of lecithin precipitate rinsed by ethanol 5 mL or chloroform 1 mL or 5 mL made the surface more hydrophobic. The visual observations of the substrates showed the surfaces of silica substrates treated with no chemicals, PEI+CNF and PEI+CNF+LP+chloroform 5 mL were clear, indicating the presence of thin film of chemicals on the surface of the silica substrate. On the other hand, the

appearance of surfaces of silica substrates treated with PEI+CNF+LP+ethanol 5 mL and PEI+CNF+LP+chloroform 1 mL were murky and shiny+colorful, respectively, indicating that the rinsing with 5 mL ethanol or 1 mL chloroform were not sufficient to remove the excess lecithin precipitate from the surface of the substrate.

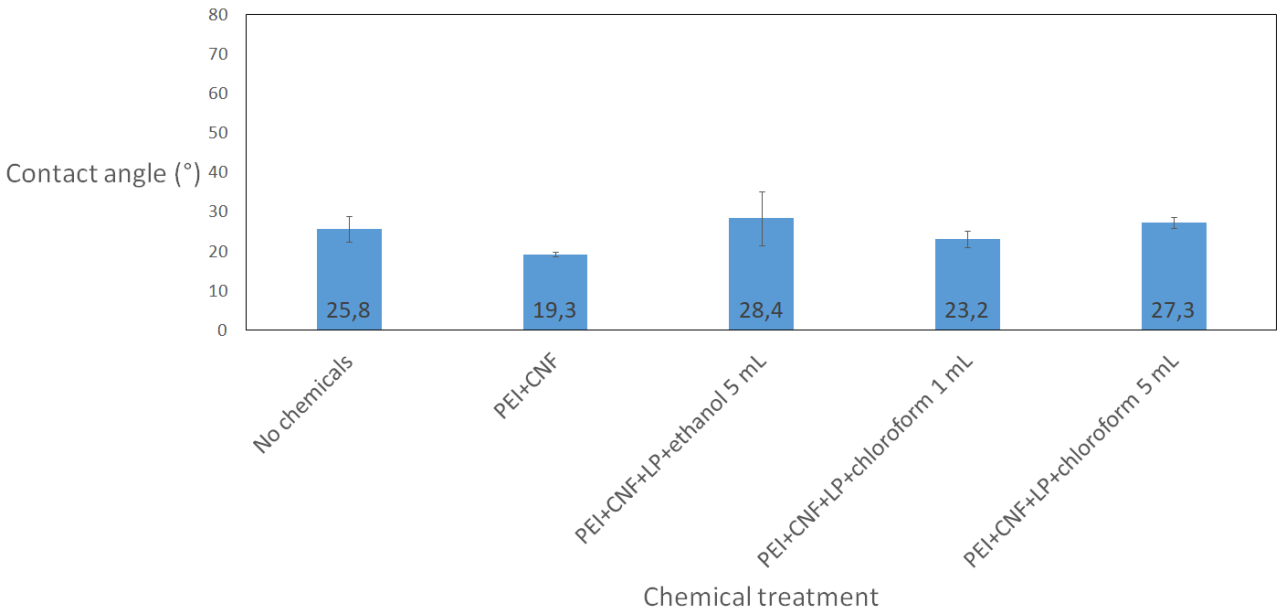

Figure 13. Contact angles of water on the substrates in the first measurement round of type 2. PEI = poly(ethyleneimine), CNF = cellulose nanofibrils and LP = lecithin precipitate.

Figures 14 and 15 show the second measurements round of CA measurements of substrates with different chemical treatments of type 1 and type 2, respectively. Figures 14 and 15, the same substrate with no chemicals (CA value of 42.5 °) was used as a reference because the reference substrate was not treated with PEI solution that would be rinsed off and then air blown or not-air blown deciding whether it would be included to either type 1 or type 2.

In Figure 14, the CA of the substrate treated with PEI+CNF was 54.0 °, which indicated that the PEI+CNF decreased the hydrophilicity of the surface compared to the substrate treated with no chemicals. This was contrary to the first measurement round of type 2 (Figure 13), which indicated that PEI+CNF increased the hydrophilicity compared to the substrate treated with no chemicals. The CA of the substrate treated with PEI+CNF+chloroform 5 mL was 46.2 °. This was lower than for the substrate treated with PEI+CNF, which indicated that chloroform increased the hydrophilicity. The CA of the substrate treated with PEI+CNF+LP+chloroform 5 mL was 38.1 °. When comparing this CA value to the substrate treated with PEI+CNF+chloroform 5 mL (CA value of 46.2 °), it seems that the LP increased the hydrophilicity. Additionally, when comparing the CA

of the substrate treated with PEI+CNF+ethanol 5 mL to the CA of the substrate treated with PEI+CNF+LP+ethanol 5 mL, it seems that the LP increased the hydrophilicity.

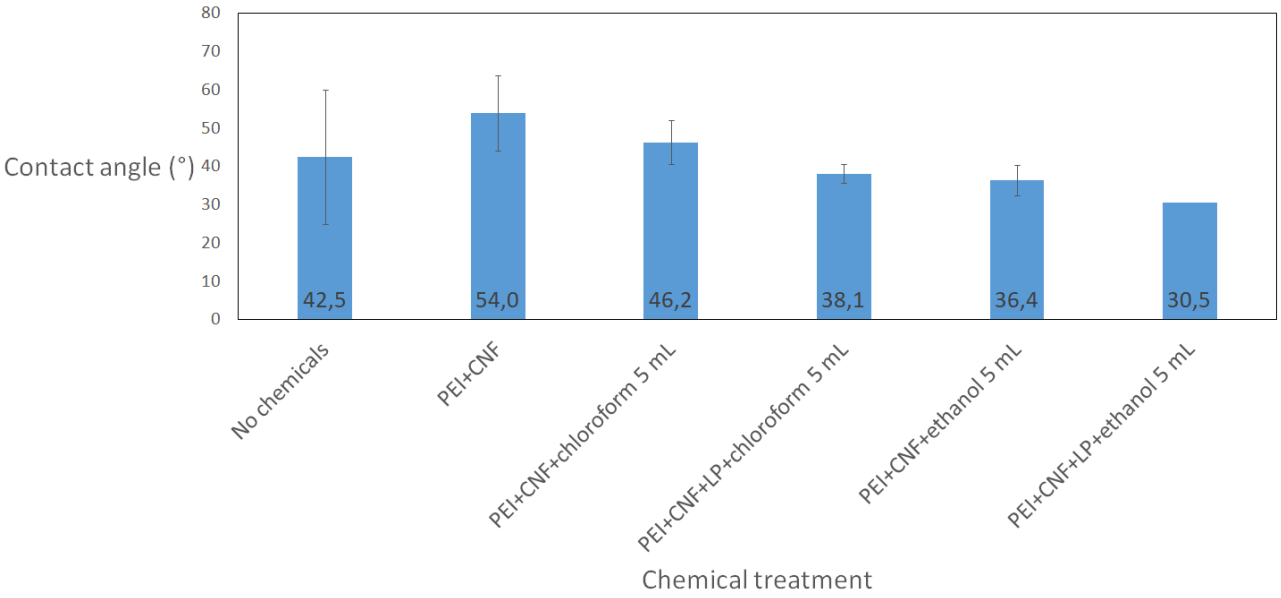

Figure 14. CA of water on the substrates in the second measurement round of type 1. PEI = poly(ethyleneimine), CNF = cellulose nanofibrils and LP = lecithin precipitate.

In Figure 15, the CA of substrate with no chemicals was 42.5 °. The CA of substrate treated with PEI+CNF was 29.6 °, which indicated that PEI+CNF increased the hydrophilicity as the wetting was enhanced. This was in agreement with the first measurement round of type 2 (Figure 13). The CA of substrates treated with PEI+CNF+chloroform 5 mL and PEI+CNF+LP+chloroform 5 mL were 34.8 ° and 35.5 °, respectively, which indicated that LP decreased hydrophilicity. The CA of the substrates treated with PEI+CNF+ethanol 5 mL and PEI+CNF+LP+ethanol 5 mL were 27.7 ° and 38.0 °, respectively, which indicated that LP decreased the hydrophilicity. According to the visual observation of the silica substrates treated with PEI+CNF+LP+ethanol 5 mL, the surface areas were ~2/3 murky and colorful, ~1/3 shiny and looked like nonrinsed liquid in two out of three substrates, and in one out of three substrates the surface area was ~2/4 murky and colorful, ~1/4 murky, ~1/4 shiny liquid looking, which indicated that the lecithin precipitate was only partially rinsed off using ethanol 5 mL in all the three substrate repeats in the second measurement round. The lecithin precipitate that would have only partially been rinsed off would have increased the contact angle though it would not have given an indication that the lecithin precipitate would have been adsorbed to the surface.

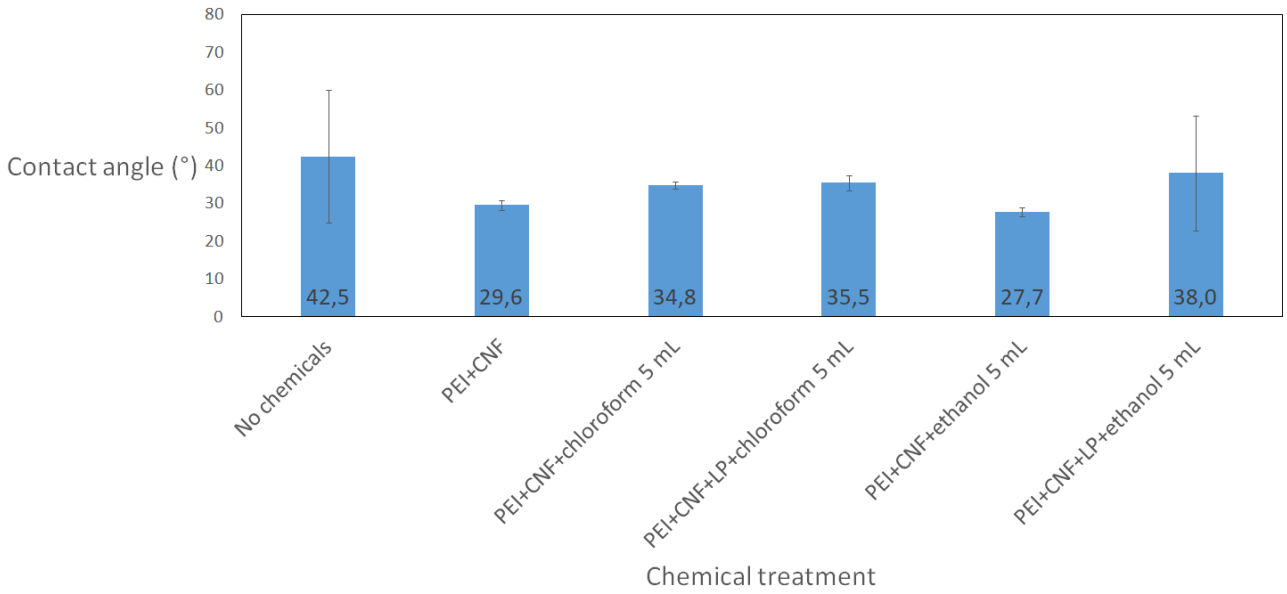

Figure 15. CA of water on the substrates in the second measurement round of type 2. PEI = poly(ethyleneimine), CNF = cellulose nanofibrils and LP = lecithin precipitate.

Figures 16 and 17 show the third measurement round of CA measurements of substrates with different chemical treatments of type 1 and type 2, respectively. In Figure 15, the CA of the substrate treated with PEI+CNF was 47.0 °. Comparing this CA value to the CA value of the substrate treated with PEI+CNF+chloroform 5 mL (50.0 °), it indicated that the chloroform 5 mL decreased the hydrophilicity. The CA value of the substrate treated with PEI+CNF+LP+chloroform 5 mL was 45.2 °, which indicated that the LP increased the hydrophilicity when comparing the value to the CA value for the substrate treated with PEI+CNF+chloroform 5 mL (50.0 °). The CA values for the substrates treated with PEI+CNF+ethanol 5 mL and PEI+CNF+LP+ethanol 5 mL were 45.5 ° and 24.4 °, respectively, which indicated that the LP increased the hydrophilicity. The CA value for the substrate treated with PEI+CNF+chloroform 1 mL was 46.5 °, which indicated that the chloroform 1 mL increased the hydrophilicity compared to the CA of the substrate treated with PEI+CNF. The CA value for PEI+CNF+LP+chloroform 1 mL was 50.5 °, which indicated that LP+chloroform 5 mL increased the hydrophilicity of the surface when compared to PEI+CNF. When comparing the substrate with PEI+CNF+chloroform 1 mL (CA value of 46.5 °) to the substrate with PEI+CNF+LP+chloroform 1 mL (CA value of 50.5 °), it indicated that the LP decreased the hydrophilicity.

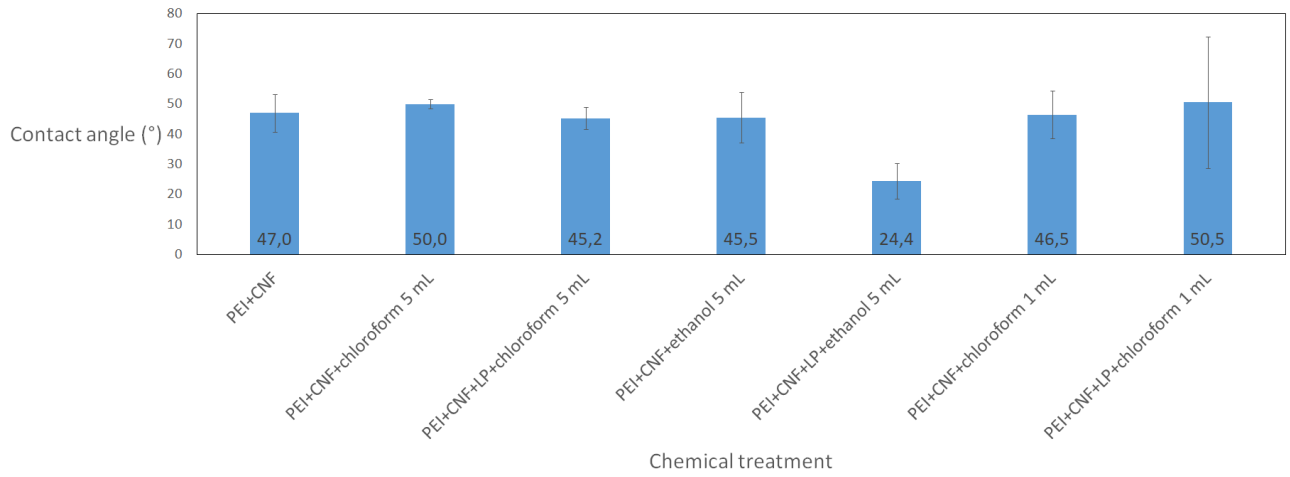

Figure 16. CA of water on the substrates in the third measurement round of type 1. PEI = poly(ethyleneimine), CNF = cellulose nanofibrils and LP = lecithin precipitate.

In Figure 17, the CA for silica substrate treated with PEI+CNF was 32.4 °. The CA for substrate treated with PEI+CNF+chloroform 5 mL was 38.3 °, which indicated that chloroform decreased the hydrophilicity. The CA of the silica substrate treated with PEI+CNF+LP+chloroform 5 mL was 29.3 °, which indicated that LP increased the hydrophilicity of the surface. Increase of hydrophilicity of LP was seen also when comparing the CA of substrates treated with PEI+CNF+ethanol 5 mL and PEI+CNF+LP+ethanol 5 mL that had the CA of 29.0 ° and 27.0 °, respectively. The CA of PEI+CNF+chloroform 1 mL was 47.0 °C. The CA for the substrate treated with PEI+CNF+LP+chloroform 1 mL was 21.8 °, which indicated that LP increased the hydrophilicity of the substrate.

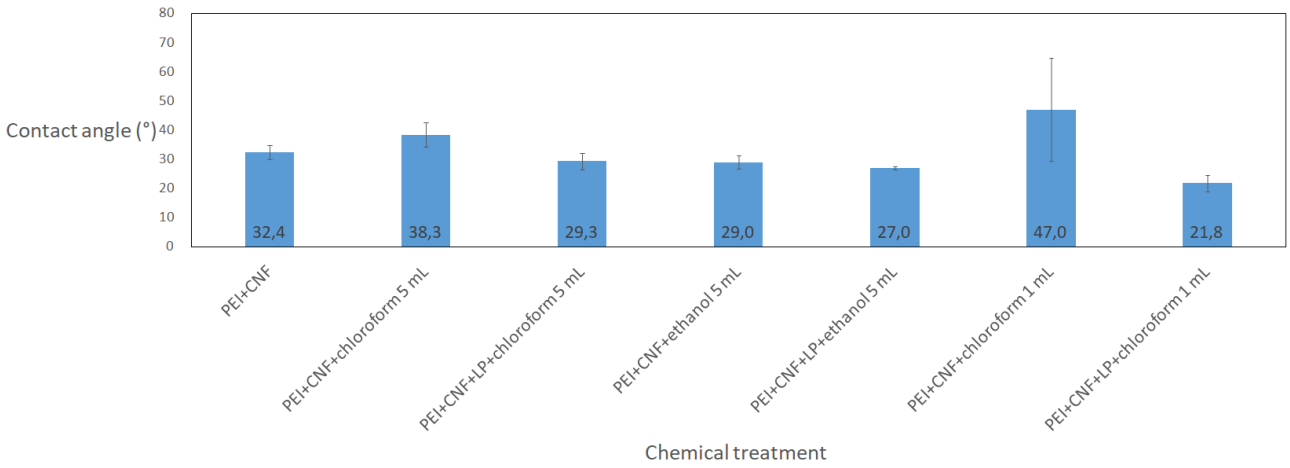

Figure 17. CA of water on the substrates of the third measurement round of type 2. PEI = poly(ethyleneimine), CNF = cellulose nanofibrils and LP = lecithin precipitate.

As a conclusion, the CA in type 2 should be evaluated to be more trustworthy compared to the type 1. This was due to the air blowing step of the wet substrates in type 2 prior to addition of CNF solution. This resulted in constant concentration of CNF. In type 2, two out of three measurements indicated that the addition of PE+CNF+LP+chloroform 5 mL to the silica surface increased the hydrophobicity of the substrate compared to the silica substrate treated with PEI+CNF. In type 2, two measurements indicated that addition LP increased the hydrophobicity of silica substrate. Overall, the immersion of the substrate into the LP, subsequent rinsing and CA measurement did not seem to be the optimal way to measure the adsorption of phospholipids on to the surface of the CNF due to the variation of the results. The hydrophilicity of the CNF may have been resulted by the surface hydroxyl groups that would have inhibited the wetting of the surface of the fiber when contacting it with the lecithin precipitate that contained hydrophobic vegetable oil and thus preventing the adsorption of phospholipid lamellar structure on the CNF surface.

3.3. Summary of the supplementary experiments

Optical microscopy studies revealed that lecithin could be solubilized into rapeseed oil, and the solubilized lecithin aggregates could be precipitated by adding moderate amount of water. Lecithin precipitate seemed to be a semi-solid material indicating that lecithin acted as a structuring agent together with water in rapeseed oil. The surface modification of nanocellulose was studied by contacting the surface with the lecithin precipitate. The hydrophobization effect of lecithin on nanocellulose surface was not clear. Several contact angle measurements indicated that the addition of LP+ethanol or chloroform to the silica surface with PEI+CNF decreased the hydrophilicity of the substrate and two measurements indicated that the addition of oily liquid containing phospholipid lamellar structures decreased the hydrophilicity of the surface. The contact angle measurement seemed not to be the optimal way to measure the adsorption phospholipids onto the surface of nanocellulose due to the variation in the results that made the interpretation difficult. More laboratory experiments should be conducted to ascertain the adsorption of phospholipids on the surface of nanocellulose. This would require for example the use of quartz crystal microbalance measurements.

4. Conclusions and future plans

The tendency of phospholipids to interact with water and free fatty acids in vegetable oil is now well understood. It was clearly shown that phospholipids are surface-active molecules, and they form different structures in vegetable oil. The properties of the structures could be controlled by changing the parameters such as temperature of the system, water concentration and free fatty acid. The most critical parameter for the solubilization of lecithin into vegetable oil seemed to be the water concentration. The solubilization of lecithin into the vegetable oil was affected by the delicate hydrophilic-hydrophobic interplay of phospholipid with water and vegetable oil together with free fatty acids. The evidence of the presence of spherical phospholipid reverse micelles in vegetable oil is still lacking, however, it can be assumed that the initial moisture of lecithin could cause the phospholipids to form elongated cylindrical reverse micelles in the oil instead of spherical reverse micelles. The solubilized phospholipids cylindrical reverse micelles in vegetable oil were shaped into lamellar phospholipid structures due to the favorable packing energetic upon addition of moderate amount of water into the vegetable oil.

It has been shown that phospholipids might be used to render the surface of nanocellulose more hydrophobic. However, according to the results, the hydrophobization effect of the surface using lecithin precipitate was not clear when performing it with contact angle measurement due to the variation in the results. For the future plans, it is recommended to study the interactions of phospholipids and nanocellulose using quartz crystal microbalance measurements. The dispersion of nanocellulose into vegetable oil should also be evaluated. In addition, the usage of nanocellulose in food products requires the evaluation of the health impacts of nanocellulose.

5. References

Andresen, M. and Stenius, P., 2007. Water-in-oil emulsions stabilized by hydrophobized microfibrillated cellulose. *Journal of Dispersion Science and Technology*. Volume 28, Issue 6, Pp. 837–844.

Angelico, R., Ceglie, A., Colafemmina, G., Lopez, F., Murgia, S., Olfsson, U. and Palazzo, G., 2005. Biocompatible lecithin organogels: structure and phase equilibria. *Langmuir*. Volume 21, Issue 1, Pp. 140–148.

Angelico, R., Ceglie, A., Olsson, U. and Palazzo, G., 2000. Phase diagram and phase properties of the system lecithin-water-cyclohexane. *Langmuir*. Volume 16, Issue 5, Pp. 2124–2132.

Bai, L., Huan, S., Xiang, W. and Rojas, O.J., 2018. Pickering emulsions by combining cellulose nanofibrils and nanocrystals: phase behavior and depletion stabilization. *Green Chemistry*, Volume 20, Issue 7, Pp. 1571–1582.

Beatrice, C.A.G., Rosa-Sibakov, N., Lille, M., Sözer, N., Poutanen, K., Ketoja, J.A., 2017. Structural properties and foaming of plant cell wall polysaccharide dispersions. *Carbohydrate Polymers*. Volume 173, Pp. 508–518.

Cantiani, R., Knipper, M. and Vaslin, S., 2002. Use of cellulose microfibrils in dry form in food formulations. United States Patent. Patent No. US 6,485,767 B1.

Cirkel, P.A. and Koper, G.J.M., 1998. Characterization of lecithin cylindrical micelles in dilute solution. *Langmuir*. Volume 14, Issue 25, Pp. 7095–7103.

Corral, M.L., Cerrutti, P., Vázquez and Califano, A., 2017. Bacterial nanocellulose as a potential additive for wheat bread. *Food hydrocolloids*. Volume 67, Pp. 189–196.

Costa, A.L.R., Gomes, A., Tibolla, H., Menegalli, F.C. and Cunha, R.L., 2018. Cellulose nanofibers from banana peels as a Pickering emulsifier: High-energy emulsification processes. *Carbohydrate Polymers*. Volume 194, Pp. 122–131.

Cui, L., Kittipongpittaya, K., McClements, D.J. and Decker, E.A., 2014. Impact of phosphatidylethanolamine reverse micelles on lipid oxidation in bulk oils. *Journal of the American Oil Chemists' Society*. Volume 91, Issue 11, Pp. 1931–1937.

Danino, D., Gupta, R., Satyavolu, J. and Talmon, Y., 2002. Direct cryogenic-temperature transmission electron microscopy imaging of phospholipid aggregates in soybean oil. *Journal of Colloid and Interface Science*. Volume 249, Issue 1, Pp. 180–186.

DeLoid, G.M., Sohal, I.S., Lorente, L.R., Molina, R.M., Pyrgiotakis, G., Stevanovic, A., Zhang, R., McClements, D.J., Geitner, N.K., Bousfield, D.W., Ng, K.W., Loo, S.C.J., Bell, D.C., Brain, J. and Demokritou, P., 2018. Reducing intestinal digestion and adsorption of fat using a nature-derived biopolymer: interference of triglyceride hydrolysis by nanocellulose. *ACS Nano*. Volume 12, Issue 7, Pp. 6469–6479.

Dufresne, A., 2012. *Nanocellulose From Nature to High Performance Tailored Materials*. Walter de Gruyter GmbH. Berlin, Germany and Boston, USA.

Elworthy, P. H., 1959. Micelle formation by lecithin in benzene. *Journal of the Chemical Society*. Pp. 813–817.

Endes, C., Camarero-Espinosa, S., Mueller, S., Foster, E.J., Petri-Fink, A., Rothen-Rutishauser, B., Weder, C. and Clift, M.J..D., 2016. A critical review of the current knowledge regarding the biological impact of nanocellulose. *Journal of Nanobiotechnology*. Volume 14, Issue 1, Article number 78.

Fujisawa, S., Togawa, E. and Kuroda, K., 2017. Nanocellulose-stabilized Pickering emulsions and their applications. *Science and Technology of Advanced Materials*. Volume 18, Issue 1, Pp. 959–971.

Golchoobi, L., Alimi, M., Shokoohi, S. and Yousefi, H., 2016. Interaction between nanofibrillated cellulose with guar gum and carboxy methyl cellulose in low-fat mayonnaise. *Journal of Texture Studies*. Volume 47, Issue 5, Pp. 403–412.

Gómez H., C., Serpa, A., Velásquez-Cock, J., Gañán, P., Castro, C., Vélez, L. and Zuluaga, R., 2016. Vegetable nanocellulose in food science: A review. *Food Hydrocolloids*. Volume 57, Pp. 178–186.

Gupta, R., Muralidhara, H.S. and Davis, H. T., 2001. Structure and phase behavior of phospholipid-based micelles in nonaqueous media. *Langmuir*, Volume 17, Issue 17, Pp. 5176–5183.

Gurtovenko, A.A., Mukhamadiarov, E.I., Kostritskii, A.Yu. and Karttunen, M., 2018. Phospholipid-cellulose interactions: insights from atomistic computer simulations for understanding the impact of cellulose-based materials on plasma membranes. *Journal of Physical Chemistry B*. Volume 122, Issue 43, Pp. 9973–9981.

Hauser, H., Pascher, I., Pearson, R.H. and Sundell, S., 1981. Preferred conformation and molecular packing of phosphatidylethanolamine and phosphatidylcholine. Biochimica et Biophysica Acta - Reviews on Biomembranes, Volume 650, Issue 1, Pp. 21–51.

Hauser, H., Pascher, I. and Sundell, S., 1980. Conformation of phospholipids. Crystal structure of a lysophosphatidylcholine analogue. *Journal of Molecular Biology*. Volume 137, Issue 3, Pp. 249–264.

He, X., Deng, H. and Hwang, H.-m., 2019. The current application of nanotechnology in food and agriculture. *Journal of Food and Drug Analysis*. Volume 27, Issue 1, Pp. 1–21.

Huan, S., Mattos, B.D, Ajdary, R., Xiang, W., Bai, L. and Rojas, O.J., 2019. Two-phase emulgels for direct ink writing of skin-bearing architectures. *Advanced Functional Materials*, DOI: 10.1002/adfm.201902990 (Article in Press).

Imai, M., Hashizaki, K., Taguchi, H., Saito, Y. and Motohashi, S., 2013. A new reverse worm-like micellar system from a lecithin, multivalent carboxylic acid and oil mixture. *Journal of Colloid and Interface Science*. Volume 403, Pp. 77–83.

Innami, S. and Yoshitaka, F., 1987. *Additive composition for foods or drugs*. United States Patent 4,659,388. Google patents.

Isaksson, B., 1951. On the lipid constituents of normal bile. *Acta Societatis Medicorum Upsaliensis*. Volume 56, Issue 5–6, Pp. 177–195.

Jendrasiak, G. L. and Hasty, J. H., 1974. The hydration of phospholipids. *Biochimica et Biophysica Acta*, Volume 337, Issue 1, Pp. 79–91.

Jendrasiak, G. L., Smith, R. L. and Shaw, W., 1996. The water adsorption characteristics of charged phospholipids. *Biochimica et Biophysica Acta*, Volume 1279, Issue 1, Pp. 63–69.

Kanamoto, R., Wada, Y., Miyajima, G. and Kito, M., 1981. Phospholipid-phospholipid interaction in soybean oil. *Journal of American Oil Chemists Society*. Volume 58, Issue 12, Pp. 1050–1053.

Khorasani, A.C. and Shojaosadati, S.A., 2017. Improvement of probiotic survival in fruit juice and under gastrointestinal conditions using pectin-nanochitin-nanolignocellulose as a novel prebiotic gastrointestinal-resistant matrix. *Applied Food Biotechnology*. Volume 4, Issue 3, Pp. 179–191.

Kleinschmidt, D.C., Roberts, B.A., Fuqua, D.L. and Melchion, J.R., 1988. *Filling-containing, dough-based products containing cellulosic fibrils and microfibrils*. United States Patent. Patent number 4,774,095. Google patents.

Koh, H.-S. and Hayama, I., 1997. *Whipping cream compositions possessing a lowered fat content and improved acid resistance and freeze resistance, and process for producing the same*. United States Patent 5,609,904.

Kostritskii, A.Yu., Tolmachev, D.A., Lukasheva, N.V. and Gurtovenko, A.A., 2017. Molecular-level insight into the interaction of phospholipid bilayers with cellulose. *Langmuir*. Volume 33, Issue 44, Pp. 12793–12803.

Lehtinen, O.-P, Nugroho, R.W.N., Lehtimaa, T., Vierros, S., Hiekkataipale, P., Ruokolainen, J., Sammalkorpi, M. and Österberg, M., 2017. Effect of temperature, water content and free fatty acid on reverse micelle formation of phospholipids in vegetable oil. *Colloids and Surfaces B: Biointerfaces*. Volume 160, Pp. 355–363

Lei, L., Ma, Y., Kodali, D., Liang, J. and Davis, H. T., 2003. Ternary phase diagram of soybean phosphatidylcholine-water-soybean oil and its application to the water degumming process. *Journal of American Oil Chemists' Society*. Volume 80, Issue 4, Pp. 383–388.

Lin, K.-W. and Lin, H.-Y., 2004. Quality characteristics of Chinese-style meatball containing bacterial cellulose (nata). *Journal of Food Science*. Volume 69, Issue 3, Pp. SNQ107–SNQ111.

McMurry, J. and Simanek, E., 2007. *Fundamentals of Organic Chemistry*. 6th edition. California, USA: Thomson Brooks/Cole. Pp. 516–517.

Oncley, J.L. and Harvie, N.R., 1969. Lipoproteins – a current perspective of methods and concepts. *Proceedings of the National Academy of Sciences of the United States of America*. Volume 64, Issue 3, Nov 1969, Pp. 1107-1118.

Pascher, I. Sundell S., and Hauser, H., 1981. Polar group interaction and molecular packing of membrane lipids. The crystal structure of lysophosphatidylethanolamine. Journal of Molecular Biology, Volume 153, Issue 3, Pp. 807–824.

Palazzo, G., 2013. Wormlike reverse micelles. *Soft Matter*. Volume 9, Issue 45, Pp. 10668–10677.

Pichot, R., Watson, R. L. and Norton, I., 2013. Phospholipids at the interface: Current trends and challenges. *International Journal of Molecular Sciences*. Volume 14, Issue 6, Pp. 11767–11794.

Rolfes S.R., Pinna, K. and Whitney, E., 2009. Undestanding Normal and Clinical Nutrition, Eighth Edition. Wadsworth, Cengage Learning. California, USA. Pp. 150–152 and 840–852.

Scartazzini, R. and Luisi, P.L., 1988. Organogels from lecithins. *Journal of Physical Chemistry*. Volume, 92, Issue 3, Pp. 829–833.

Schurtenberger, P., Scartazzini, R., Magid, L.J., Leser, M.E. and Luisi, P.L., 1990. Structural and dynamic properties of polymer-like reverse micelles. *Journal of Physical Chemistry*. Volume 94, Issue 9, Pp. 3695–3701.

Small, D. M., 1986. *The Physical Chemistry of Lipids, From Alkanes to Phospholipides*, New York, USA: Plenum Press.

Stephens, R.S., Westland, J.A. and Neogi, A.N., 1990. *Method of using bacterial cellulose as a dietary fiber component*. Patent Number 4,960,763, Date of Patent Oct. 2, 1990.

Subramanian, R., Ichikawa, S., Nakajima, M., Kimura, T., Maekawa, T., 2001. Characterization of phospholipid reverse micelles in relation to membrane processing of vegetable oils. *European Journal of Lipid Science and Technology*. Volume 103, Issue 2, Pp. 93–97.

Sun, L., Chen, W., Liu, Y., Li, J. and Yu H., 2015. Soy protein isolate/cellulose nanofiber complex gels as fat substitutes: rheological and textural properties and extent of cream imitation. *Cellulose*. Volume 22, Issue 4, Pp. 2619–2627.

Szuhaj, B. F., 2005. Lecithins, Volume 3, In Shadidi, F. (Ed.) *Bailey's Industrial Oil and Fat products*. 6th edition. New Jersey, USA: John Wiley & Sons, Inc., Publication.

Turbak, A.F., Snyder, F.W. and Sandberg, K.R., 1982. *Food products containing microfibrillated cellulose*. United States Patent 4,341,807. Google patents.

Turbak, A.F., Snyder, F.W. and Sandberg, K.R., 1983. *Suspensions containing microfibrillated cellulose*. United States Patent 4,378,381. Google patents.

Vartiainen, J., Pöhler, T., Sirola, K., Pylkkänen, L., Alenius, H., Hokkinen, J., Tapper, U., Lahtinen, P., Kapanen, A., Putkisto, K., Hiekkataipale, P., Eronen, P., Ruokolainen, J. and Laukkanen A., 2011. Health and environmental safety aspects of friction grinding and spray drying of microfibrillated cellulose. *Cellulose*. Volume, 18, Issue 3, Pp. 775–786.

Velásquez-Cock, J., Serpa, A., Vélez, L., Gañán, P., Gómez Hoyos, C., Castro, C., Duizer, L., Goff, H.D., Zuluaga, R., 2019. Influence of cellulose nanofibrils on the structural elements of ice cream. *Food hydrocolloids*. Volume 87, Pp. 204–213.

Walde, P., Giuliani, A. M., Boicelli, C. A. and Luisi, P. L., 1990. Phospholipid-based reverse micelles. *Chemistry and Physics of Lipids*. Volume 53, Issue 4, Pp. 265–288.

Zhang, J., Chang, P., Zhang, C., Xiong, G., Luo, H., Zhu, Y., Ren, K., Yao, F. and Wan Y., 2015. Immobilization of lecithin on bacterial cellulose nanofibers for improved biological functions. *Reactive & Functional Polymers*. Volume 91–92, Pp. 100–107.